Acta Pharmaceutica Sinica B 2022;12(3):1305−1321

Chinese Pharmaceutical Association
Institute of Materia Medica, Chinese Academy of Medical Sciences

Acta Pharmaceutica Sinica B

www.elsevier.com/locate/apsb
www.sciencedirect.com

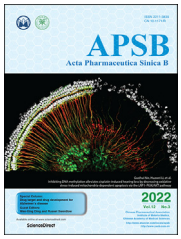

ORIGINAL ARTICLE

Inhibiting DNA methylation alleviates cisplatin-induced hearing loss by decreasing oxidative stress-induced mitochondria-dependent apoptosis *via* the LRP1−PI3K/AKT pathway

Yingzi He[a,b,†], Zhiwei Zheng[a,b,†], Chang Liu[a,b,†], Wen Li[a,b], Liping Zhao[a,b], Guohui Nie[e,*], Huawei Li[a,b,c,d,*]

[a]*ENT Institute and Otorhinolaryngology Department of Eye & ENT Hospital, State Key Laboratory of Medical Neurobiology and MOE Frontiers Center for Brain Science, Fudan University, Shanghai 200031, China*
[b]*NHC Key Laboratory of Hearing Medicine (Fudan University), Shanghai 200031, China*
[c]*Institutes of Biomedical Sciences, Fudan University, Shanghai 200032, China*
[d]*The Institutes of Brain Science and the Collaborative Innovation Center for Brain Science, Fudan University, Shanghai 200032, China*
[e]*Department of Otolaryngology and Institute of Translational Medicine, Shenzhen Second People's Hospital/the First Affiliated Hospital of Shenzhen University Health Science Center, Shenzhen 518035, China*

Received 3 June 2021; received in revised form 29 October 2021; accepted 1 November 2021

KEY WORDS

Cisplatin;
DNMT;
Apoptosis;
Hair cell;
Spiral ganglion neurons;
RG108;

Abstract Cisplatin-related ototoxicity is a critical side effect of chemotherapy and can lead to irreversible hearing loss. This study aimed to assess the potential effect of the DNA methyltransferase (DNMT) inhibitor RG108 on cisplatin-induced ototoxicity. Immunohistochemistry, apoptosis assay, and auditory brainstem response (ABR) were employed to determine the impacts of RG108 on cisplatin-induced injury in murine hair cells (HCs) and spiral ganglion neurons (SGNs). Rhodamine 123 and TMRM were utilized for mitochondrial membrane potential (MMP) assessment. Reactive oxygen species (ROS) amounts were evaluated by Cellrox green and Mitosox-red probes. Mitochondrial respiratory function evaluation was

Abbreviations: 5-mC, 5-methylcytosine; ABR, auditory brainstem response; DNMT, DNA methyltransferase; EdU, 5-ethynyl-2′-deoxyuridine; HCs, hair cells; IHCs, inner hair cells; LRP1, low-density lipoprotein receptor-related protein 1; MMP, mitochondrial membrane potential; OCRs, oxygen consumption rates; OHCs, outer hair cells; PI, propidium iodide; ROS, reactive oxygen species; SGNs, spiral ganglion neurons; TUNEL, terminal deoxynucleotidyl transferase-mediated dUTP nick-end-labeling.

*Corresponding authors. Tel.: +86 21 64377134.
E-mail addresses: nieguohui@email.szu.edu.cn (Guohui Nie), hwli@shmu.edu.cn (Huawei Li).
[†]These authors made equal contributions to this work.

Peer review under responsibility of Chinese Pharmaceutical Association and Institute of Materia Medica, Chinese Academy of Medical Sciences.

https://doi.org/10.1016/j.apsb.2021.11.002

Mitochondrial dysfunction;
ROS

performed by determining oxygen consumption rates (OCRs). The results showed that RG108 can markedly reduce cisplatin induced damage in HCs and SGNs, and alleviate apoptotic rate by protecting mitochondrial function through preventing ROS accumulation. Furthermore, RG108 upregulated BCL-2 and downregulated APAF1, BAX, and BAD in HEI-OC1 cells, and triggered the PI3K/AKT pathway. Decreased expression of low-density lipoprotein receptor-related protein 1 (LRP1) and high methylation of the LRP1 promoter were observed after cisplatin treatment. RG108 treatment can increase LRP1 expression and decrease LRP1 promoter methylation. In conclusion, RG108 might represent a new potential agent for preventing hearing loss induced by cisplatin *via* activating the LRP1-PI3K/AKT pathway.

1. Introduction

Cisplatin represents a potent chemotherapeutic molecule with wide use in a broad spectrum of malignant diseases[1]. Unfortunately, ototoxicity, neurotoxicity, and nephrotoxicity are serious undesirable effects of cisplatin that quite limit its application[2]. It is primarily admitted cisplatin profoundly injures HCs in the organ of Corti and severely affects SGNs in the inner ear, resulting in irreversible, accumulative, bilateral, and sensorineural hearing loss[1,3,4]. Although the mechanisms behind cisplatin-associated ototoxicity have not been completely explained, it may mainly involve ROS accumulation in the inner ear, causing a significant increase in lipid peroxidation, consumption of intracochlear antioxidants, and calcium influx, subsequently inducing apoptosis[5]. Several studies examining antioxidative reagents, such as glutathione, *N*-acetyl-cysteine, and sodium thiosulfate, have been performed in animals[6–8].

Epigenetics assesses gene regulation by post-translational modifications of the chromatin structure without changing the DNA sequence, which has important functions in diverse cellular processes[9–11]. During the past few years, understanding epigenetic mechanisms of transcriptional regulation has been considered an important element of auditory pathologies. Recently, many studies have shown that epigenetic modifications, such as histone acetylation and methylation, play significant roles in the phenotype and function of cochlear sensory cells in many models in pathologic conditions and discovered some epigenetic targeted drugs for preventing and treating ototoxic-induced hearing loss. For instance, Wang et al.[12] found that histone deacetylase inhibitors could reverse cisplatin-associated regulatory effects on apoptosis-related genes and protect against cisplatin induced ototoxicity. Yu et al.[13] demonstrated that elevated expression of H3K9me2 is associated with ototoxic-induced HC damage and hearing loss in a mouse model and demonstrated an otoprotective impact of G9a inhibition by treatment with BIX 01294 both *in vitro* and *in vivo*, which was regulated, at least in part, through inhibition of caspase-3 mediated apoptosis. However, the detailed mechanism is still not well elucidated. A recent study revealed an essential role for protein arginine methyltransferase 6 in mediating cisplatin-associated hearing loss, inhibiting this histone-modifying enzyme by a known inhibitor, EPZ020411, provided otoprotection through inhibition of the mitochondria-dependent apoptotic pathway[14]. These findings indicate that epigenetic modifications are mechanisms involved in the death of cochlear sensory cells and reveal the critical role of epigenetic agents in cell survival of various types of hearing loss.

DNA methylation represents a significant epigenetic modification that regulates gene expression. It plays crucial role in maintaining chromosome structure, genomic imprinting, X-chromosome inactivation, and the occurrence and development of many human diseases[15,16]. DNA methylation transfers a methyl group to 5-cytosine under catalysis by DNMT[17,18]. There are three major DNMT family members in mammals, including DNMT1, DNMT3a, and DNMT3b. DNMT1 is the dominant member in proliferating cells, which maintains methylation pattern through DNA replication; meanwhile, DNMT3a and DNMT3b perform *de novo* methylation of DNA[19,20]. DNA methylation is usually associated with gene silencing, while DNA demethylation stimulates gene expression[21,22]. Currently, the evidence about the effects of DNMTs on inner ear development and hearing pathology is scarce. Studies in mouse utricle sensory epithelia-derived progenitor cells identified increased expression levels of HC and prosensory genes upon treatment with the DNMT suppressor 5-aza-2′-deoxycytidine, which induced inner ear progenitor cells to differentiate into sensory HC-like cells, providing a new epigenetic strategy for stem cell therapy[23,24]. Moreover, in an aminoglycoside-induced deafened mouse model, the DNMT inhibitor 5-aza could promote the regeneration of cochlear HCs[25]. However, the role and mechanism of DNA methylation in ototoxic insults-induced hearing loss are not elucidated.

RG108 is a new non-nucleoside small molecule DNMT inhibitor, which was identified in virtual screening of 1553 molecules extracted from the NCI database. It has been reported that RG108 induces DNA demethylation without cytotoxicity compared with other DNMT inhibitors such as 5-aza-dC, because its action does not need to be incorporated into DNA[26–28]. Recently, RG108, as a universal antioxidant, was shown to play critical roles in free radical quenching, antioxidant recycling, and metal chelation[29]. This work aimed to assess the involvement of DNA methylation in ototoxicity caused by cisplatin as well as the potential effects of RG108 in alleviating cisplatin-associated hearing loss and to explore the underlying mechanisms of RG108's effects.

2. Materials and methods

2.1. Organotypic culture of postnatal murine cochleae

Experimental procedures involving animals had approval from the Shanghai Medical Experimental Animal Administrative Committee. Cochlear specimens from postnatal day (P) 2 C57BL/6 mice were dissected from the surrounding tissue and placed in

culture dishes with Cell-Tak (BD Biosciences, San Jose, CA, USA) coating. Explant incubation was performed in DMEM/F12 containing N2/B27 (Thermo Fisher Scientific, Waltham, MA, USA) and ampicillin in a humid environment with 5% CO_2 at 37 °C overnight before treatment.

2.2. HEI-OC1 cell culture

HEI-OC1 cell culture was carried out in high-glucose DMEM (Thermo Fisher Scientific) containing 5% FBS (Thermo Fisher Scientific) at 33 °C in a 5% CO_2 atmosphere. Cell subculture used 0.25% trypsin/EDTA (Thermo Fisher Scientific), and was performed at 80% confluence.

2.3. Drug treatments

RG108 and LY294002 were purchased from Selleck Chemicals (Houston, TX, USA) and initially dissolved in DMSO (Sigma−Aldrich, St. Louis, MO, USA) to 10 mmol/L stock solutions and then applied at final concentrations (RG108: 10, 50, and 100 μmol/L; LY294002: 20 μmol/L). Cisplatin (Sigma−Aldrich) was freshly dissolved in culture medium (1 mmol/L) and further diluted for all assays.

2.4. Animal treatments

Age-matched 7−8-week both sexes of wild-type adult C57BL/6 mice weighing 18 to 20 g were examined. To test the protective effect of RG108 *in vivo*, 1 mL pre-warmed sterile saline was intraperitoneally injected one day preceding cisplatin and/or RG108 administration. Then, RG108 was injected intraperitoneally at 10 mg/kg; 2 h later, 30 mg/kg cisplatin was administered by i.p. injection once. After cisplatin administration, mice from all groups (control, cisplatin, RG108, RG108 + cisplatin) received 1 mL of pre-warmed saline intraperitoneally twice daily for seven days for alleviating kidney toxicity and dehydration. Following the final saline injection, mice recovered for additional seven days before post-cisplatin treatment ABR tests. The dose of cisplatin tested and the procedure was based on a study assessing mice with hearing loss[30].

2.5. Cell viability detection

CCK-8 (Sigma−Aldrich) was utilized to assess cell viability. Briefly, HEI-OC1 cells in each group underwent washing with pre-warmed PBS, followed by addition of CCK-8 solution for 3 h. Absorbance was measured on a microplate reader (Bio-Rad Laboratories, Hercules, CA, USA) at 450 nm. The positive control well underwent the same procedure with no cells, and the negative control well had no drug treatment. Each group was assessed in triplicate.

2.6. Flow cytometry analysis for Annexin V/PI

FITC Annexin V Apoptosis Detection Kit (BD Biosciences Pharmingen, San Diego, CA, USA) was utilized for apoptosis quantitation as directed by the manufacturer. In brief, after PBS wash, the cells were resuspended in 1 × binding buffer, which was followed by adding 5 μL each of Annexin V-FITC and propidium iodide (PI) and incubation at ambient for 15 min shielded from light. About 10,000−20,000 cells/group were assessed on a FACS Calibur system (BD Biosciences) and evaluated with FlowJo 7.6. Assays were performed in triplicate with three independent experiments.

2.7. Caspase-3/7 assay

HEI-OC1 cells were washed in serum-free DMEM and stained with 5 μmol/L caspase-3/7 green detection reagent (Thermo Fisher Scientific) in a medium without serum (37 °C, 30 min). Fluorescence microscopy and flow cytometry were performed for analysis.

2.8. Terminal deoxynucleotidyl transferase-mediated dUTP nick-end-labeling (TUNEL) assay

TUNEL assay was carried out according to the protocols of *In Situ* Cell Death Detection Kit (Roche, Indianapolis, IN, USA). After staining with DAPI and required antibodies, a Leica confocal laser scanning microscope (Leica TCS SP8, Leica Microsystems GmbH, Wetzlar, Germany) was utilized for visualization.

2.9. ROS and MMP assay

ROS amounts were assessed with Cellrox green and Mitosox-red (Thermo Fisher Scientific). Upon treatment and PBS wash, the cells underwent staining with 5 μmol/L Cellrox green or 5 μmol/L Mitosox-red in pre-warmed serum-free DMEM shielded from light for 30 min. Fluorescence intensity was measured using a Leica SP8 confocal fluorescence microscope and a FACS Calibur system. All assays were repeated at least three times.

MMP was examined by assessing Rhodamine 123 (Thermo Fisher Scientific) and TMRM (Thermo Fisher Scientific). Upon treatment, cells underwent incubation with 1 μmol/L Rhodamine 123 or 20 nmol/L TMRM (30 min, 37 °C) in the dark. A Leica SP8 confocal fluorescence microscope and a FACS Calibur system were utilized for analysis. All assays were repeated at least three times.

2.10. Seahorse analysis of mitochondrial respirometry

Cellular OCR was assessed on a Seahorse XF96 Extracellular Flux Analyzer (Seahorse Bioscience, North Billerica, MA, USA), as recommended by the manufacturer. HEI-OC1 cells underwent seeding in triplicate on Seahorse XF96 cell culture microplates (3×10^4 cells/well). After overnight incubation, HEI-OC1 cells were administered RG108 with or without cisplatin, followed by 24 h incubation. After washing, DMEM was supplemented for subsequent assessment. For OCR assay, 2.0 μmol/L oligomycin (a complex V suppressor) was loaded to port A, while 0.5 μmol/L FCCP was injected in port B; a mixture of rotenone and antimycin A (complex I and III suppressors) was loaded to port C at 100 nmol/L and 1 μmol/L, respectively. During sensor calibration, cells underwent incubation at 37 °C in a non-CO_2 incubator in 180 μL XF base medium containing 10 mmol/L glucose, 10 mmol/L pyruvate, and 2 mmol/L L-glutamine (pH 7.4). A calibrated XFp Extracellular Flux Analyzer for Mito Stress Test was employed for assessment, and data analysis used the Seahorse XF analysis software based on total protein.

2.11. ABR measurements

ABR testing was completed before each treatment to ensure normal hearing ability, as described in a previous study[13]. Mice underwent anesthesia with ketamine (100 mg/kg, i.p.) and xylazine sodium (25 mg/kg, i.p.) and kept warm during ABR measurements. A TDT System III apparatus (Tucker-Davis

Technologies Inc., Alachua, FL, USA) was employed for hearing threshold assessment at 8, 16, 24, and 32 kHz, respectively.

2.12. Immunofluorescence

Fixed cochleae and cells underwent permeabilization (1% Triton X-100 in PBS [PBST]; 30 min), blocking (10% donkey serum in PBST; 1 h) and incubation with primary antibodies overnight at 4 °C. For cochlear cryosections, cochlear specimens were rinsed with PBS (0.01 mol/L), decalcified with 10% EDTA at 4 °C and immersed in 15% sucrose/PB (0.1 mol/L) solution for 30 min, followed by overnight immersion in 30% sucrose/PB (0.1 mol/L) at 4 °C. The cochlear specimens then underwent embedding in optimal cutting temperature (OCT) compound, freezing and sectioning at 10−12 μm. After blocking (10% donkey serum, 1 h), the samples were incubated with primary antibodies targeting myosin7a (1:500, Proteus Biosciences, Ramona, CA, USA), parvalbumin (1:500, Abcam, Cambridge, MA, USA), Tuj-1 (1:1000, Biolegend, San Diego, CA, USA), neurofilament (1:1000, Abcam), 5-methylcytosine (5-mC, 1:500, Abcam), cleaved-caspase3 (C-caspase3, 1:500, Cell Signaling Technology, Beverly, CA, USA), C-terminal binding protein (CtBP2, 1:1000, BD Transduction Laboratories, BD Biosciences, San Jose, CA), SOX2 (1:1000, R&D Systems, Minneapolis, MN, USA), and APAF1 (1:500, Abcam). Then, they underwent incubation with secondary fluorescent antibodies for 1 h shielded from light. DAPI (4′,6-diamidino-2-phenylindole; Sigma−Aldrich) was used for 10 min counterstaining. For phalloidin staining, fixed cochlear specimens underwent incubation with Alexa Fluor 488 phalloidin (Thermo Fisher Scientific) for 30 min shielded from light and DAPI counterstaining. To label proliferating cells, 5-ethynyl-2′-deoxyuridine (EdU) was supplemented at 10 μmol/L for three days. EdU detection utilized the Click-iT™ Plus EdU Alexa Fluor 488 Imaging Kit (Thermo Fisher Scientific). Specimens were visualized under a Leica SP8 confocal fluorescence microscope.

2.13. Immunoblot

Samples underwent lysis with chilled RIPA buffer (Beyotime Institute of Biotechnology, Nanjing, China) containing a protease inhibitor cocktail (Sigma−Aldrich) at 4 °C for 30 min. The lysed samples underwent centrifugation (12,000 × *g*, 20 min) at 4 °C. The BCA protein assay kit (Beyotime Institute of Biotechnology) was utilized for total protein quantitation in supernatants. Equal amounts of total protein were resolved by SDS-PAGE followed by transfer onto polyvinylidene difluoride (PVDF) membranes (Millipore, Merck KGaA, Darmstadt, Germany). Blocking was carried out with 5% skim milk in TBS with 0.1% Tween 20 (TBST) for 1 h, followed by successive incubations with primary (overnight) and HRP-linked secondary (1:5000; 1 h) antibodies. The SuperSignal West Dura chemiluminescent substrate kit (Thermo Fisher Scientific) was utilized for detection, and data analysis used ImageJ (Broken Symmetry Software, National Institutes of Health, Bethesda, MD, USA). Experiments were repeated at least three times. The primary antibodies used targeted BAX (1:500, Cell Signaling Technology), BCL-2 (1:500, Cell Signaling Technology), BAD (1:500, Cell Signaling Technology), cleaved-caspase3 (C-caspase3, 1:500, Cell Signaling Technology), AKT (1:500, Cell Signaling Technology), phospho-AKT at Ser473 (1:500, Cell Signaling Technology), APAF1 (1:1000, Abcam), LRP1 (1:1000, Abcam), DNMT1 (1:1000, Abcam) and GAPDH.

2.14. siRNA transfection

For the transfection of siRNAs, HEI-OC1 cells underwent culture on plates for 24 h and administered *Lrp1*-or control siRNA using Lipofectamine 2000 (Thermo Fisher Scientific) for an additional 24 h, following the manufacturer's directions. The transfected cells were administered cisplatin or control medium, inducted for 24 h and harvested for analysis. The following siRNAs were used: mouse *Lrp1* siRNA1 (targeting AAGCATCTCAGTAGACTATCA)[31], mouse *Lrp1* siRNA2 (targeting AACTTCTTAAACTCATAGCTT), and mouse *Lrp1* siRNA3 (targeting AAGCAGTTTGCCTGCAGAGAC).

2.15. RNA-seq and quantitative-PCR

RNA extraction utilized the RNeasy Mini Kit (Qiagen, Valencia, CA, USA), as directed by the manufacturer. A NanoDrop 2000 spectrophotometer (Thermo Fisher Scientific) was employed for determining RNA purity and amounts. RNA integrity assessment used an Agilent 2100 Bioanalyzer (Agilent Technologies, Santa Clara, CA, USA). TruSeq Stranded mRNA LT Sample Prep Kit (Illumina, San Diego, CA, USA) was employed for library building as directed by the manufacturer. An Illumina HiSeq X Ten platform was used for library sequencing, generating 150-bp paired-end reads. Raw reads (fastq format) were firstly processed with Trimmomatic[32], and low quality reads were removed to obtain clean reads. Differential expression analysis utilized the DESeq (2012) R package. $P < 0.05$, fold change > 2 and FDR < 0.01 indicated significant differential expression. KEGG pathway enrichment analyses of DEGs were performed with R on the basis of hypergeometric distribution.

2.16. Pyrosequencing analysis

DNA methylation assays were carried out with bisulfite-treated DNA and PCR-pyrosequencing-based quantitation. Bisulfite conversion utilized 2 μg of genomic DNA obtained from HEI-OC1 cells with Qiazol (Qiagen) and 0.1 μmol/L citrate ethanol. Next, PCR was carried out in 25 μL reactions containing 0.5 μmol/L of each primer. One primer underwent biotinylation for purifying the final PCR product with Sepharose beads. Finally, 10 μL of each PCR product underwent pyrosequencing on a PyroMark Q48 ID Pyrosequencing System (Qiagen) using 4 μmol/L of the sequencing primer. Primers for pyrosequencing are listed in Supporting Information Table S1.

2.17. HC, SGN, and cochlear ribbon synapse counts

For HC quantification, cells labelled with myosin7a and showing normal nuclei were considered surviving HCs. The entire cochlea was divided into three turns, including the apex, middle, and base. The surviving HCs were counted in 200 μm long strip encompassing the area from base to apex. Only the middle part of the explant (40%−60% from the apex) was examined for apoptosis assessment. For SGN quantification, SGNs were immuno-labeled with anti-Tuj-1 antibody, and all fibers were quantified in the middle portion of each explant. Tuj-1-labelled soma with a large round nucleus was counted. To quantify ribbon synapses, cochlear specimens were stained with anti-CtBP2 antibody, and the number of CtBP2 per IHC field was obtained.

2.18. Statistical analysis

One-way analysis of variance (ANOVA) was used for comparing groups. Data from at least three independent assays are mean ± standard error of mean (SEM). GraphPad Prism6 (GraphPad, San Diego, CA, USA) was employed for data analysis. $P < 0.05$ indicated statistical significance.

3. Results

3.1. DNMT1 inhibition protects HCs from cisplatin-related injury in vitro

To determine the appropriate cisplatin exposure time for inducing HC damage, cochlear specimens from P2 WT C57BL/6 mice were cultured overnight to allow for recovery before incubation with cisplatin at 30 μmol/L for 24 or 48 h[14]. After 72 h recovery following cisplatin administration, HCs were labelled with antibody against myosin7a. The results showed that cisplatin time-dependently decreased the amounts of HCs. Cisplatin at 30 μmol/L for 24 h extensively killed both inner HCs (IHCs) and outer HCs (OHCs) in cochlear basal and middle turns (Supporting Information Fig. S1). Increasing the exposure time to 48 h resulted in a marked loss of HCs in the basal, middle and apical turns of the cochlea, remarkably disrupting the normal architecture of the cochlea (Fig. S1A and S1B). Thus, cisplatin at 30 μmol/L for 24 h was selected for establishing the cochlear HC injury model.

To assess RG108's effect on cisplatin-related ototoxicity, murine cochlear specimens were pretreated with RG108 at increasing concentrations (10, 50, and 100 μmol/L) for 2 h, incubated for 24 h with cisplatin, and allowed to recover for an additional 72 h before staining for myosin7a to label HCs. As shown in Fig. 1A, controls show no loss of HCs with the typical one and three intact rows of IHCs and OHCs, respectively; however, cisplatin administration resulted in an obvious HC loss in a base-to-apex gradient. In contrast, pretreatment of explants with RG108 remarkably decreased cisplatin-related HC loss. Cisplatin-associated HC loss was attenuated by RG108 beginning at 50 μmol/L, with the efficacy increasing with concentration and surviving HCs reaching a peak at 100 μmol/L of RG108 (Fig. 1B). RG108 by itself did not induce any apparent morphological change in HCs at 100 μmol/L (Fig. 1A). Therefore, 100 μmol/L RG108 was selected for subsequent murine cochlear experiments. To assess whether RG108's protective effects on cisplatin-induced HC loss were related to the inhibition of DNA methylation, DNA methylation levels in mouse cochlear specimens were evaluated by 5-mC staining. The results indicate that cisplatin administration induced DNA hypermethylation in HCs compared with undamaged HCs, while RG108 pretreatment reduced this cisplatin-induced DNA hypermethylation (Supporting Information Fig. S2A). Furthermore, we analyzed DNMT1 protein levels by Western blot analysis, and DNMT1 amounts were increased by cisplatin, in accordance with DNA hypermethylation levels in the genome (Fig. S2B and S2C).

To demonstrate the important role of RG108 in apoptosis, cleaved-caspase3 immunostaining and TUNEL assay were performed to detect cochlear cell apoptosis (Fig. 1C and D). The numbers of positive cleaved-caspase3 (4.71 ± 0.62) and TUNEL (4.95 ± 0.77) cells were starkly elevated upon cisplatin exposure, suggesting that the apoptotic pathway was mainly responsible for cisplatin-induced HC damage. In contrast, RG108 pretreatment dramatically reduced cleaved-caspase3- (0.21 ± 0.14) and TUNEL- (0.35 ± 0.17) positive cells. To determine whether proliferation is a direct result of RG108 treatment, we treated cultured cochlea explants with EdU together with or without RG108 for three days after cisplatin treatment. Although RG108 treatment caused a significant uptake of EdU, almost no myosin7a^{+}/EdU^{+} cells were observed in both cisplatin and RG108 + cisplatin groups (Supporting Information Fig. S3). These results strongly indicate that RG108 treatment improved survival in cochlear HCs without affecting HC regeneration.

3.2. Inhibition of DNMT1 protects SGNs from cisplatin-related damage in vitro

To establish an SGN injury model, the cultured middle turns of murine cochleae underwent treatment with 30 μmol/L cisplatin for 24 or 48 h, and the SGN explants were allowed to recover for 72 h before staining with Tuj-1 to label SGNs. The results show that although HCs were significantly inhibited by treatment with 30 μmol/L cisplatin for 24 h, a slight SGN damage was detected in the explants (Fig. S1C and S1D). When the cisplatin administration time was extended to 48 h, the densities of SGN somas and radial nerve fibers were significantly decreased at 30 μmol/L; most SGN somas significantly decreased, and most nerve fibers were absent; multiple blebs and debris were found on the remaining nerve fibers (Fig. S1C and S1D). Therefore, cisplatin at 30 μmol/L for 48 h was selected for the SGN injury model.

To assess whether RG108 exerts comparable protective effects on SGNs against cisplatin damage, murine SGN explants were pretreated with RG108 at 100 μmol/L for 2 h, and challenged for 48 h with or without cisplatin. Immunostaining results in Fig. 2A show that cisplatin significantly decreased neurite densities and SGN soma compared with the undamaged control, whereas the addition of RG108 induced statistically significant elevations in the numbers of neurites and SGN somas. In terms of morphology, SGNs in the RG108 group had large, round or oval cell bodies, different from those of the cisplatin-only group showing small somas. The neurite lengths of explants obtained in the presence of RG108 were also longer than those observed when SGNs were treated with cisplatin only (Fig. 2C–E). Addition of RG108 alone to explants under normal conditions did not induce any apparent change in SGN amount or morphology, suggesting RG108 itself did not damage SGNs. Next, to examine the effect of RG108 on apoptosis, cochlear SGNs were co-labelled by Tuj-1, TUNEL, and myosin7a staining (Fig. 2B). A large number of TUNEL-positive cells were found in SGN explants after cisplatin treatment. In contrast, cochlear explants pretreated with RG108 combined with cisplatin had fewer TUNEL-positive, apoptotic cells than the cisplatin-only group. These data suggest that RG108 treatment protects SGN against cisplatin-induced apoptosis.

3.3. Inhibition of DNMT1 abrogates cisplatin-associated hearing loss in vivo

To evaluate RG108's protective effects *in vivo*, both sexes of C57BL/6 mice were administered RG108 at 10 mg/kg body weight and injected 30 mg/kg cisplatin (i.p.) 2 h later, according to a previous report; 14 saline-treated animals without cisplatin administration constituted the control group. ABR was determined 14 days later (Fig. 3A). As shown in Fig. 3B, ABR thresholds were significantly increased in mice that received cisplatin administration compared with controls not administered cisplatin, confirming that cisplatin-induced hearing loss. Using the same

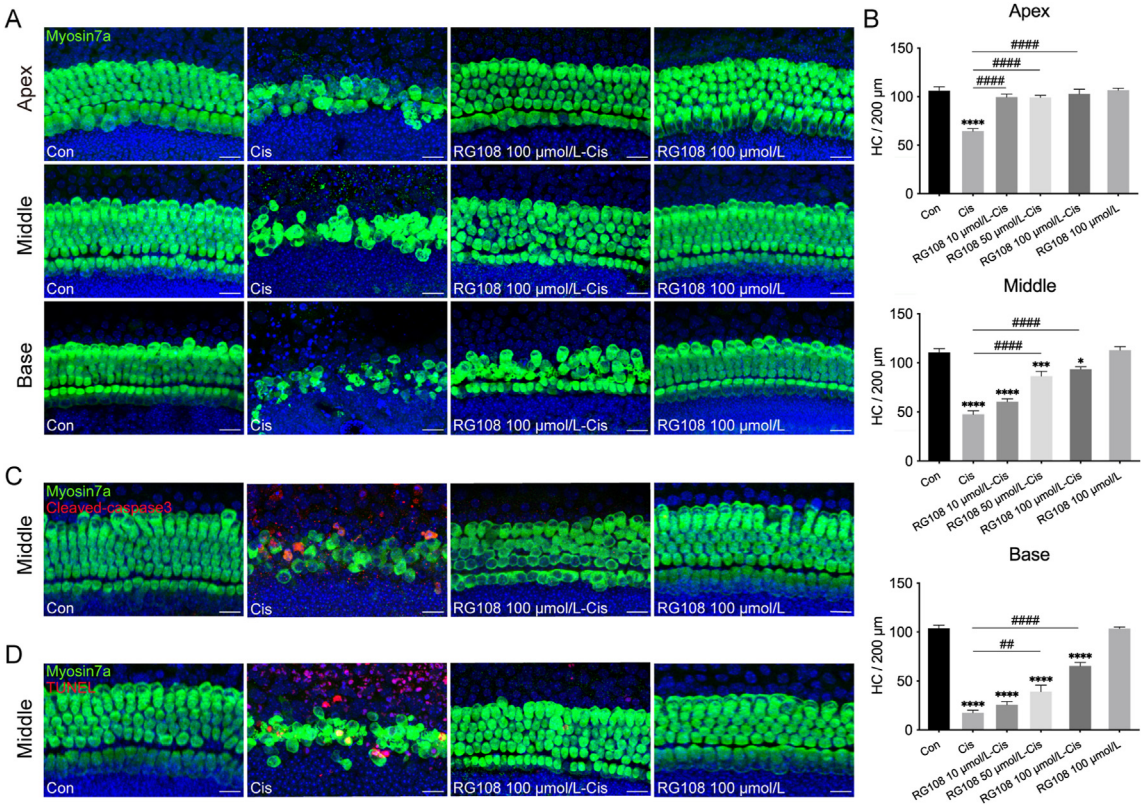

Figure 1 Effects of RG108 on cisplatin-induced cochlear HC loss *in vitro*. (A) Representative confocal photomicrographs showing the apical, middle and basal regions of the cochlear explants treated with medium alone (Con), RG108, cisplatin (Cis), or cisplatin in combination with RG108 (RG108-Cis) for 24 h and immunolabeled for myosin7a (green) and DAPI (blue). Scale bars = 20 μm. (B) The illustration of HC counting (myosin7a, green) (n = 6−12 cochleae). (C) and (D) Immunofluorescence staining for myosin7a (green) and cleaved-caspase3 (red) (C) or myosin7a (green) and TUNEL (red) (D) in the middle turns of the cochleae from each treatment group. Scale bars = 20 μm. Data are shown as mean ± SEM; $^{*}P < 0.05$, $^{***}P < 0.001$, $^{****}P < 0.0001$ *vs.* Con; $^{\#\#}P < 0.01$, $^{\#\#\#\#}P < 0.0001$ *vs.* Cis. Con, control; Cis, cisplatin; HC, hair cell.

schedule described above, mice that received an injection of RG108 before cisplatin administration exhibited significantly reduced threshold elevation (Fig. 3B), demonstrating the protective effects of RG108 on cisplatin-related hearing loss. Of note, changes in ABR thresholds in the control and RG108 (10 mg/kg) alone groups were less than 5 dB at every frequency tested, suggesting that RG108 alone did not affect hearing ability.

After ABR testing, the cochleae were harvested, fixed immediately, and dissected into apical, middle, and basal sections; HCs underwent staining with myosin7a and Alexa Fluor 488 linked-phalloidin (Fig. 3C). The survival numbers of myosin7a-positive HCs in all three turns in the cisplatin group were markedly reduced compared to control values (Fig. 3C and D). However, pretreatment with RG108 starkly reduced HC loss, especially in basal and middle turns, compared with the cisplatin-only group (Fig. 3C and D). This finding was confirmed by immunofluorescence of cochlear sections. Cisplatin administration decreased the numbers of OHCs at both basal and middle cochlear sections compared with controls, while RG108 treatment protected OHCs from cisplatin-induced damage (Fig. 3E).

Next, SGNs were stained with anti-Tuj-1 antibody, and surviving SGNs were counted (Fig. 3F). Quantitative analysis of the apical, middle, and basal turns demonstrated that the mean density of SGNs was starkly reduced in the cisplatin group compared with the control group, while the RG108 pretreatment group showed remarkably higher amounts of surviving SGNs (Fig. 3G). In the cisplatin group, more positive TUNEL signals were observed in SGNs (Fig. 3H). However, almost no positive TUNEL signal was found in SGNs from the RG108 + cisplatin group.

To examine the role of RG108 in maintaining adequate cochlear innervation, neurofilament (NF) and myosin7a co-immunostaining was carried out. In control mice, most axons contacted OHCs; however, significant loss of auditory nerve axons from IHCs to OHCs in the cochlear middle turns was observed in the cisplatin group. On the other hand, most fibers targeted OHCs in the RG108 + cisplatin group (Fig. 4A and C). Quantitatively, NF-positive projections to the OHC region were more abundant in the RG108 + cisplatin group than in the cisplatin-only group (Fig. 4B). To test whether the reduction in fiber density resulted in a change in the number of synapses, the latter were stained with anti-C-terminal binding protein 2 (CtBP2) antibody, which target the major presynaptic ribbon protein with specific staining of both presynaptic ribbons and inner HC nuclei (Fig. 4D). CtBP2 staining in the control group displayed small puncta studding the basolateral surface of IHCs; the average numbers of anti-CtBP2 per IHC in basal, middle, and apical turns of control cochleae were 17.5 ± 0.7, 17.5 ± 0.4 and 16.7 ± 0.3, respectively; these values were significantly reduced to 3.7 ± 0.4, 6.3 ± 0.6, and 7.9 ± 0.4 upon cisplatin injury, respectively (Fig. 4E). RG108 protected against the loss of CtBP2 staining (14.3 ± 0.9, 16.4 ± 0.6 and 15.1 ± 0.6, respectively). Furthermore, we assessed wave I amplitudes and latencies, which reflect the activity of auditory nerve

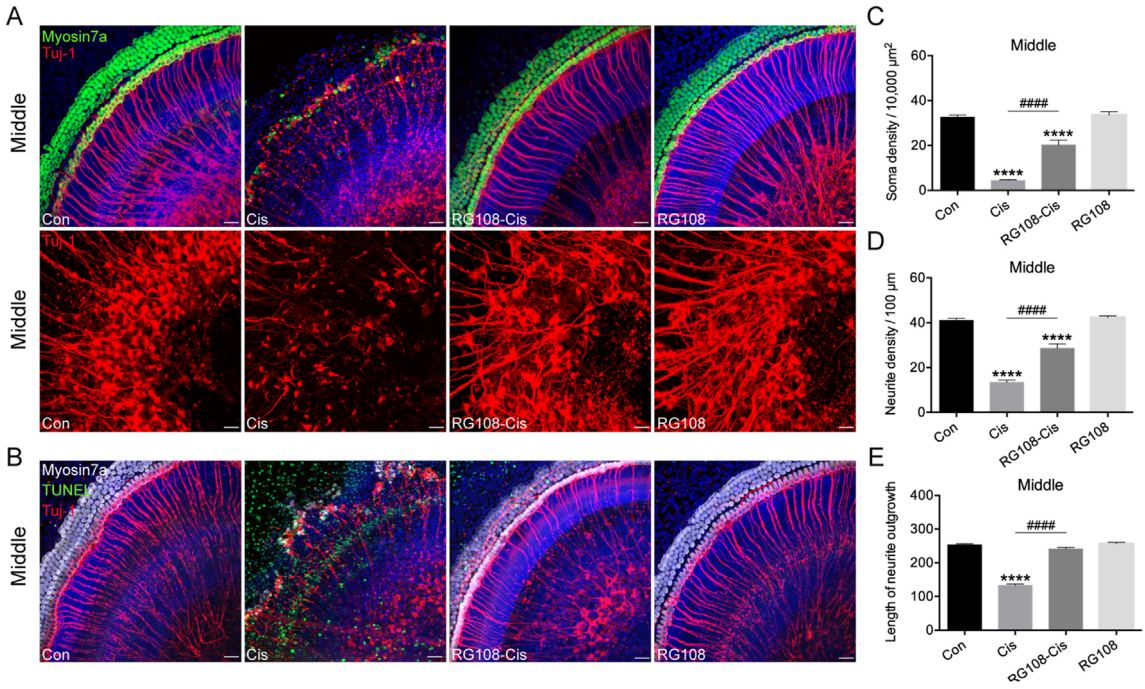

Figure 2 Effects of RG108 on cisplatin-induced cochlear SGNs damage *in vitro*. (A) Immunofluorescence staining for Tuj-1 (red) and myosin7a (green) in the middle turns of the cochleae from each treatment group. Scale bars = 20 μm. (B) Immunofluorescence staining for Tuj-1 (red), myosin7a (white) and TUNEL (green) in the middle turns of the cochleae. Scale bars = 20 μm. (C)−(E) Quantification analysis of SGN soma densities, neurite densities, and the length of neurite outgrowth from the middle turns of cochlear explants for all treatment conditions (each group, $n = 12$ SGN explants). Data are shown as mean ± SEM; $^{****}P < 0.0001$ *vs.* Con; $^{\#\#\#\#}P < 0.0001$ *vs.* Cis. Cis, cisplatin; SGNs, spiral ganglion neurons.

fibers. Our data suggest that cisplatin administration significantly diminished wave I amplitudes and elevated latencies compared with normal controls, whereas RG108 pretreatment alleviated this cisplatin-associated decreased amplitudes and increased latencies (Fig. 4F and G). Jointly, the above findings suggested RG108 starkly reduced cisplatin-related loss of neuronal fibers and synapses and promoted SGN survival.

3.4. RG108 suppresses cisplatin-associated HEI-OC1 cell apoptosis

To evaluate protective effect of RG108 on cisplatin-related cytotoxicity, HEI-OC1 cells were pretreated with a series of RG108 concentrations (10, 50, and 100 μmol/L) for 2 h before administration of 30 μmol/L cisplatin for 24 h, and examined for viability by CCK-8. The results in Fig. 5A show that HEI-OC1 cell pretreatment with 100 μmol/L RG108 markedly increased cell viability compared to the cisplatin alone group; thus, 100 μmol/L RG108 was selected as the optimal dose for subsequent HEI-OC1 cell experiments. Next, the effect of RG108 on cisplatin-related HEI-OC1 cell apoptosis was determined flow-cytometrically upon staining with Annexin V-FITC/PI. As illustrated in Fig. 5B, the apoptosis rate increased dramatically in the cisplatin group compared with control cells (48.23% *vs.* 4.037%). However, RG108 combined with cisplatin decreased this value to 22.6% (Fig. 5C). As apoptotic protease activating factor 1 (APAF1) represents a vital regulator of the mitochondrial apoptosis pathway, modulating cytochrome *c*-dependent procaspase-9 activation, resulting in caspase-3 activation, APAF1 staining was performed. As shown in Fig. 5D, increased APAF1 staining was detected in cisplatin-treated HEI-OC1 cells; however, staining signals were starkly decreased after RG108 pretreatment. Immunoblot confirmed that the proapoptotic related proteins BAX, BAD, and APAF1 were upregulated, while BCL-2 (an anti-apoptotic protein) amounts were decreased in HEI-OC1 cells following cisplatin administration; these effects were significantly reversed by pretreatment with RG108 (Supporting Information Fig. S4). We also evaluated RG108's effect on HEI-OC1 cell apoptosis by caspase-3/7 and TUNEL staining (Fig. 5E−I). Confocal microscopy shows that cells administered cisplatin only had strong caspase-3/7 and TUNEL signals compared with the control group, but RG108 pretreated cells had markedly reduced amounts of caspase-3/7 and TUNEL-positive cells compared with the cisplatin alone group. Taken together, Annexin/PI, TUNEL, and caspase-3/7 staining showed that cisplatin-induced apoptosis was alleviated in the presence of RG108.

3.5. RG108 protects mitochondrial function in HEI-OC1 cells from cisplatin damage

ROS level is a significant oxidative stress indicator in HCs, playing essential roles in cisplatin-related damage[33]. Here, the effect of RG108 on cisplatin-associated elevation of intracellular ROS was examined using the fluorescence probe Cellrox green. Immunohistochemistry and flow cytometry data indicate that excessive intracellular ROS amounts in cisplatin injured HEI-OC1 cells compared to the control group (Fig. 6A−C), while RG108 pretreatment significantly reversed the cisplatin-induced elevation of ROS levels. Additionally, mitochondrial ROS amounts were

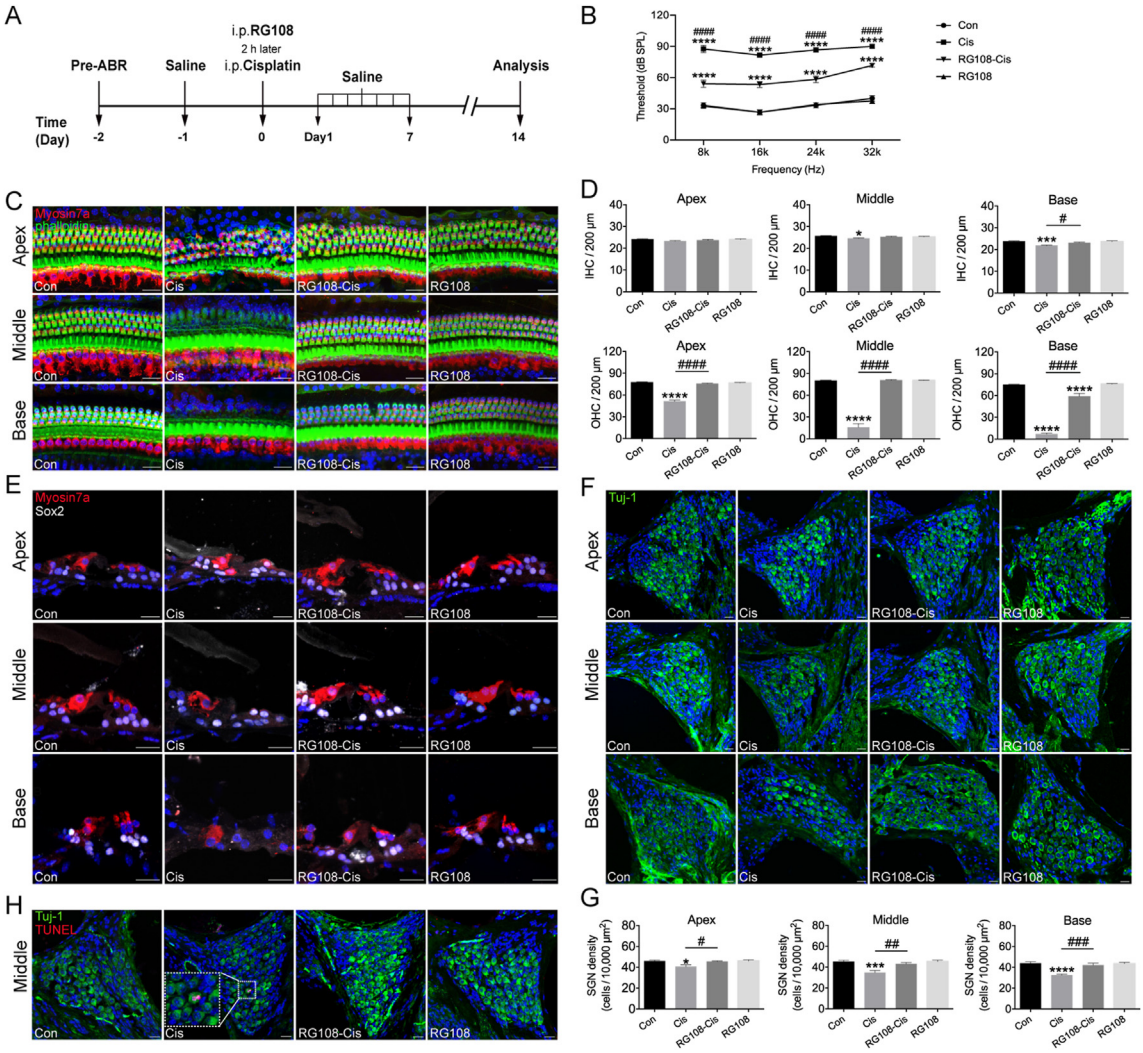

Figure 3 Effects of RG108 on cisplatin-induced hearing loss *in vivo*. (A) Experimental workflow. (B) ABR thresholds at 8, 16, 24, 32 kHz were measured 14 days after injection of saline (Con), cisplatin (Cis), cisplatin plus 10 mg/kg RG108 (RG108-Cis), and 10 mg/kg RG108 only (RG108) (each group, $n = 6$ mice). (C) Immunostaining with myosin7a (red) and Alexa Fluor 488 phalloidin (green) in the apical, middle, and basal turns of cochleae from different groups. Scale bars = 20 μm. (D) The illustration of HC counting (myosin7a, red) ($n = 9$–13 cochleae). (E) Immunostaining with myosin7a (red) and Sox2 (white) in the inner ear sections of mice from different group. Scale bars = 20 μm. (F) Representative images of Tuj-1 (green) staining of SGNs at apical, middle, and basal turns of the cochlea from different groups. Scale bar = 20 μm. (G) The illustration of SGN counting (Tuj-1, green) ($n = 10$ cochleae). (H) Immunostaining with Tuj-1 (green) and TUNEL (red) in the middle turns of SGNs from different groups. Scale bars = 20 μm. The data represent mean ± SEM; $^{*}P < 0.05$, $^{***}P < 0.001$, $^{****}P < 0.0001$ *vs.* Con; $^{\#}P < 0.05$, $^{\#\#}P < 0.01$, $^{\#\#\#}P < 0.001$, $^{\#\#\#\#}P < 0.0001$ *vs.* Cis. IHCs, inner hair cells; OHCs, outer hair cells.

measured with the fluorescence probe Mitosox-red (Fig. 6D). Flow cytometry reveals that cisplatin-related elevation of mitochondrial ROS was starkly reduced after RG108 pretreatment (Fig. 6E and F). The above findings indicate that RG108 may play an anti-apoptotic role by suppressing ROS increase in HEI-OC1 cells treated with cisplatin. Given the involvement of mitochondrial ROS as an important target of RG108 during HC protection, we further sought to determine whether the pro-survival effect of RG108 was accompanied by mitochondrial function improvement. The MMP ($\Delta\Psi$m) was assessed using the Rhodamine 123 and TMRM probes. As demonstrated in Fig. 6G and J, cisplatin starkly decreased Rhodamine 123 and TMRM fluorescence at 24 h compared to control cells, which was reversed by pretreatment with RG108 (Fig. 6H–I and K–L).

We also evaluated oxidative phosphorylation in HEI-OC1 cells, using the Seahorse XF Cell Mito Stress Test, monitoring the OCR, a measure of mitochondrial respiration[34]. Four parameters of mitochondrial function in HEI-OC1 cells were assessed, including basal respiration rate, ATP-linked respiration, maximal respiration, and spare respiratory capacity (Fig. 6M). As demonstrated in Fig. 6N, cisplatin-induced significant reductions in all these indexes in HEI-OC1 cells, and these changes were partially attenuated by pretreatment with RG108 (Fig. 6O–R). In sum, these findings suggest that improved mitochondrial function in HEI-OC1 cells could be

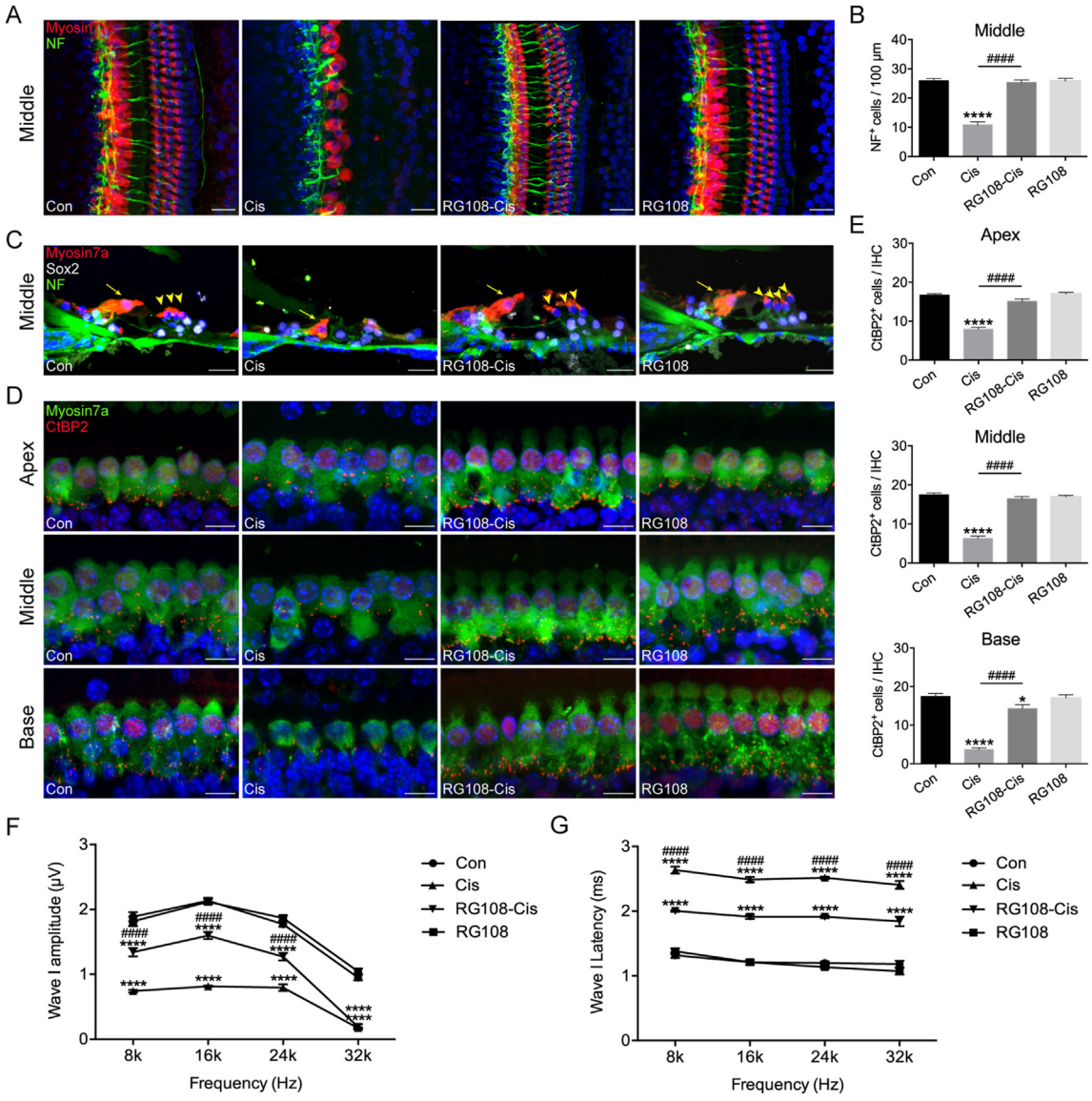

Figure 4 Effects of RG108 on cisplatin-induced hearing loss *in vivo*. (A) Immunostaining with myosin7a (red) and NF (neurofilament, green) in the middle turns of cochleae from different groups. Scale bars = 20 μm. (B) The illustration of cochlear nerve terminals counting (NF, green) (n = 8 cochleae). (C) Analysis for cochlear nerve terminals (NF, green), HCs (myosin7a, red), and supporting cells (SOX2, white) in mice for each condition. Images were taken from the middle turn of the cochlea in the inner ear sections. The yellow arrowheads point to three rows of outer HCs, and the yellow arrow indicates an inner HC. Scale bar = 20 μm. (D) Immunostaining with myosin7a (green) and CtBP2 (red) in the apical, middle, and basal turns of cochleae from different groups. Scale bars = 10 μm. (E) The illustration of CtBP2 counting (n = 6 cochleae). (F)−(G) ABR wave I amplitudes and latencies were measured 14 days after injection of saline (Con), cisplatin (Cis), cisplatin plus 10 mg/kg RG108 (RG108-Cis), and 10 mg/kg RG108 only (RG108) (each group, n = 6 mice). The data represent mean ± SEM. $^{*}P < 0.05$, $^{****}P < 0.0001$ *vs.* Con; $^{\#\#\#\#}P < 0.0001$ *vs.* Cis.

one of the important mechanisms explaining the protective effect of RG108 in cells damaged by cisplatin.

3.6. Inhibition of DNMT1 mainly activates the PI3K/AKT signaling pathways and alleviates mitochondrial damage in HCs injured by cisplatin

In order to explore the molecular mechanism by which RG108 regulates survival in HCs, we analyzed transcriptome-wide changes in HEI-OC1 cells after cisplatin damage by RNA sequencing (RNA-seq). As shown in Fig. 7A, RNA-seq analysis identified 1009 differential genes (765 upregulated and 244 downregulated) between the cisplatin and RG108 + cisplatin treatment groups. To further confirm the potential role of RG108, KEGG analysis was carried out. The top 20 regulated signaling pathways are shown in Fig. 7B, among which had remarkable changes, the apoptosis-related genes were the most prominent (Fig. 7C). Of these, the PI3K/AKT signaling pathway had the highest enrichment. To confirm RNA-seq data, seven PI3K/AKT signaling-related genes were selected and examined by qPCR, which corroborated the sequencing findings (Fig. 7D).

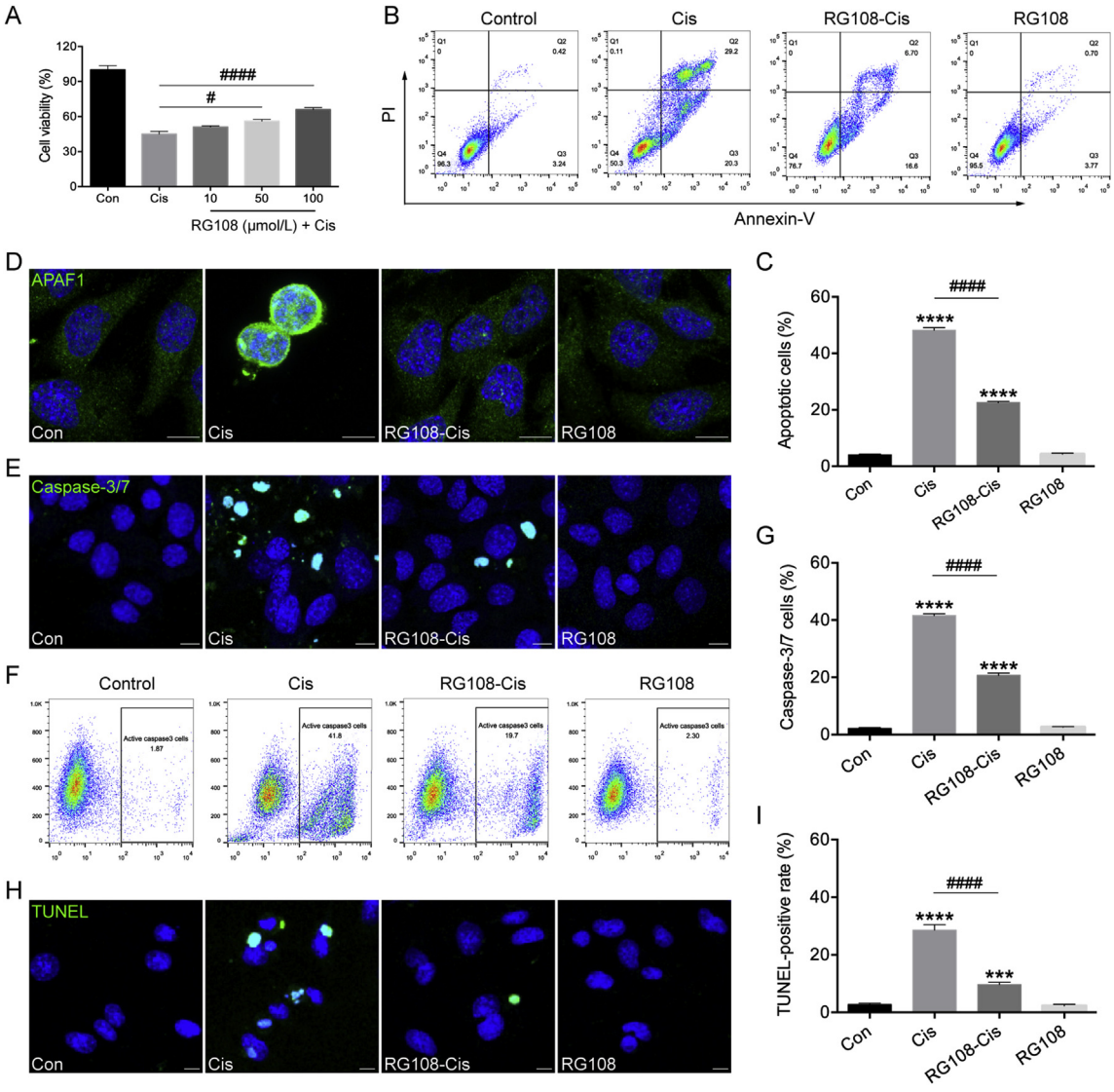

Figure 5 Effects of RG108 on cisplatin-induced apoptosis in HEI-OC1 cells. (A) Cell viability was determined by the CCK-8 assay. (B) and (C) Flow cytometry analysis of RG108 on cell apoptosis induced by cisplatin. Apoptotic cells were detected by Annexin V-FITC/PI kit. (D) Representative images of APAF1 staining in HEI-OC1 cells. (E) Representative images of caspase-3/7 staining in HEI-OC1 cells. (F) Flow cytometry analysis of caspase-3/7 in HEI-OC1 cells. (G) Quantitative changes in the caspase-3/7 were analyzed by flow cytometry data. (H) Representative images of TUNEL staining in HEI-OC1 cells. (I) Quantification of TUNEL positive cells. TUNEL staining was quantified by counting the TUNEL staining-positive cells and then normalizing to the total cell number in each image. Four different fields were selected from a coverslip, and three independent experiments were performed. Scale bars = 10 μm. Data are shown as mean ± SEM. $^{***}P < 0.001$, $^{****}P < 0.0001$ *vs.* Con; $^{\#}P < 0.05$, $^{\#\#\#\#}P < 0.0001$ *vs.* Cis.

Next, to confirm the role of the PI3K/AKT pathway in RG108-mediated protective effect in HEI-OC1 cells, protein levels of AKT, and phosphorylated AKT (activated AKT; p-AKT) were investigated by Western blot. Notably, decreased AKT and p-AKT amounts were observed in cisplatin challenged cells, whereas RG108 treatment significantly elevated AKT and p-AKT levels (Fig. 8A). The role of PI3K/AKT signaling in mediating the protective effect of RG108 was next assessed in HCs. To this end, HEI-OC1 cells were pretreated with the PI3K/AKT suppressor LY294002 (20 μmol/L)[35] for 2 h before cisplatin treatment. Cell viability measurement used the CCK-8 kit; as demonstrated in Fig. 8B, LY294002 blocked the protective effect of RG108 in HEI-OC1 cells damaged by cisplatin, and cell viability was starkly reduced in comparison with cells not pretreated with LY294002 (Fig. 8B). Moreover, a mouse model showed that the LY2940024 treatment also robustly abolished the apoptosis-inhibitory effect of RG108 in HCs and SGNs following the cisplatin challenge (Fig. 8C−F). The above findings suggest that PI3K/AKT signaling is involved, at least partially, in the protective effect of RG108 against cisplatin-related ototoxicity.

3.7. *LRP1 knockdown suppresses the protective effect of RG108*

LRP1 has anti-inflammatory and anti-apoptotic roles in disease[36]. Previous data have shown that LRP1 activation exerts anti-apoptotic effects and improves neurological function through

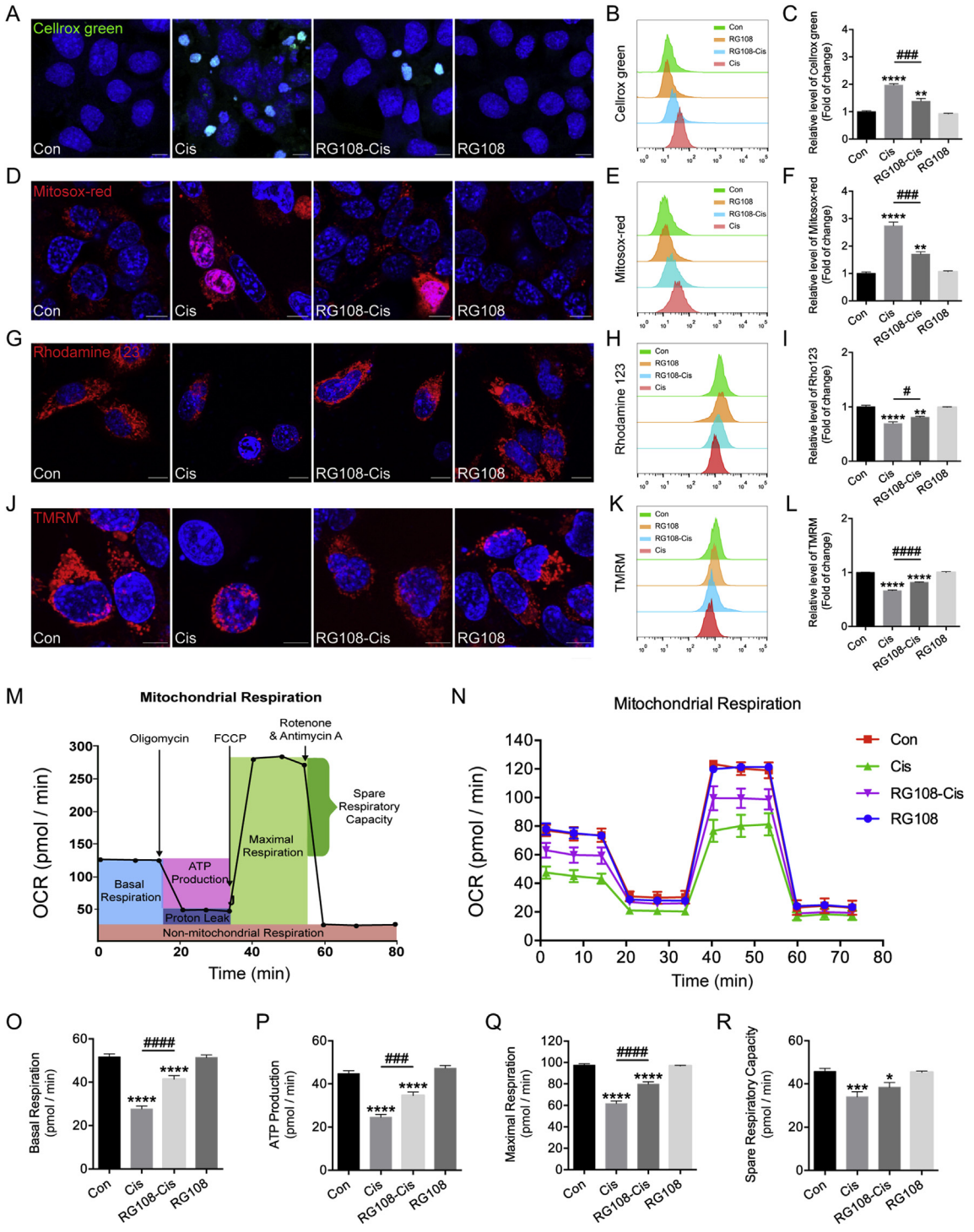

Figure 6 Effects of RG108 on ROS production and mitochondrial functions in HEI-OC1 cells after cisplatin injury. (A)−(C) Representative images and quantitative changes of Cellrox green in HEI-OC1 cells from each group. (D)−(F) Representative images and quantitative changes of Mitosox-red in HEI-OC1 cells from each group. (G)−(I) Representative images and quantitative changes of Rhodamine 123 in HEI-OC1 cells from each group. (J)−(L) Representative images and quantitative changes of TMRM in HEI-OC1 cells from each group. Scale bar = 10 μm. (M)−(R) Seahorse mitochondrial function assay. The data shown are representative of three independent seahorse runs. Data are shown as mean ± SEM. $^{*}P < 0.05$, $^{**}P < 0.01$, $^{***}P < 0.001$, $^{****}P < 0.0001$ *vs.* Con; $^{\#}P < 0.05$, $^{\#\#\#}P < 0.001$, $^{\#\#\#\#}P < 0.0001$ *vs.* Cis.

PI3K/AKT signaling in a rat model of subarachnoid hemorrhage[37]. Our RNA-seq data reveal *Lrp1* was starkly downregulated in cisplatin-treated cells compared with the control group, while RG108 could markedly increase the mRNA levels of *Lrp1* (Fig. 9A). We hypothesized that RG108 may be an important parameter regulating LRP1 in HEI-OC1 cells based on these findings. To test the above hypothesis, an immunoblot was carried out to examine LRP1 protein amounts in HEI-OC1 cells. After

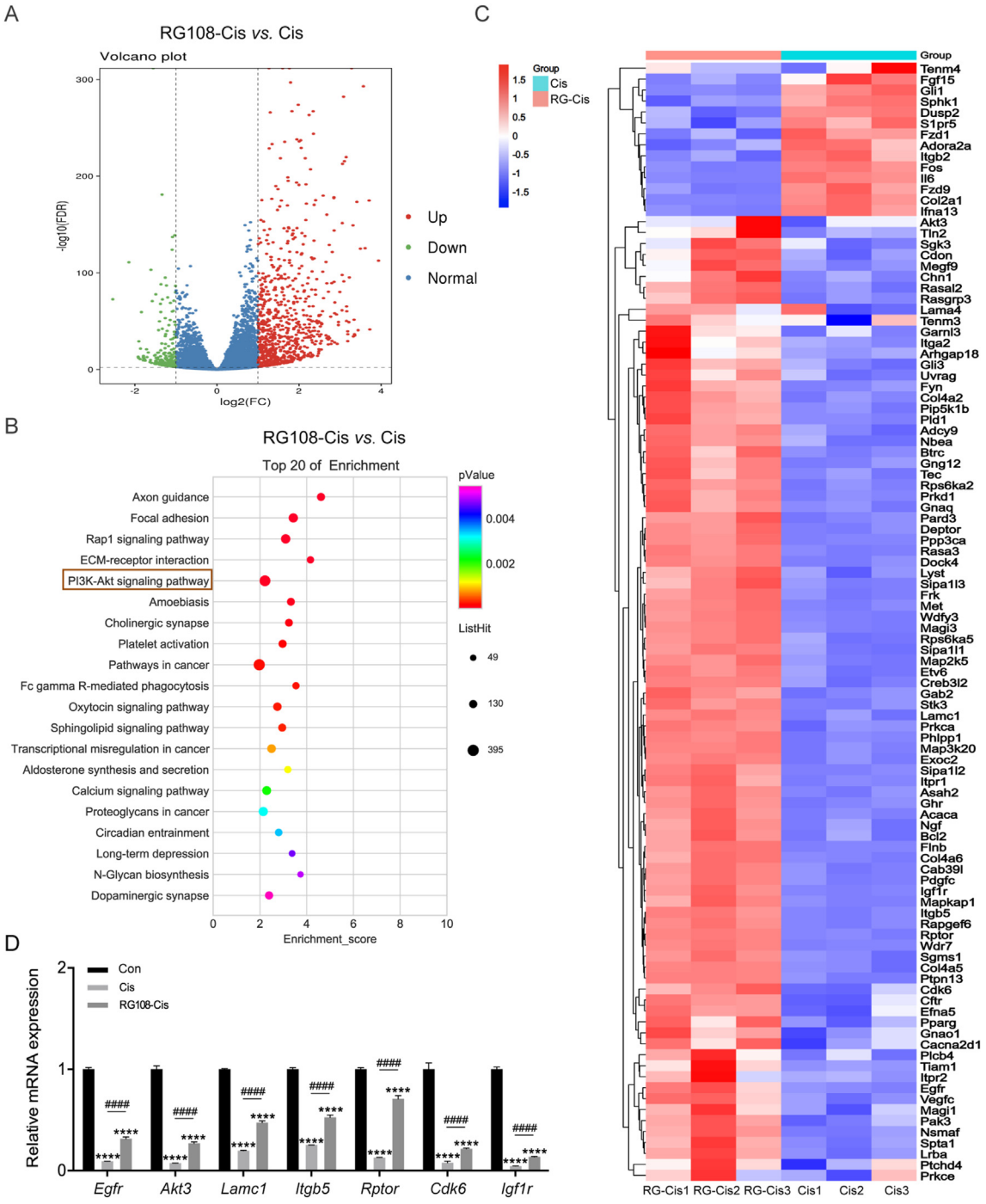

Figure 7 Effect of RG108 on the transcriptome profiles of HEI-OC1 cells in response to cisplatin stimulation. (A) Volcano plot showing dysregulated genes between cisplatin and RG108 + cisplatin groups. (B) KEGG based gene function analysis showing the top 20 most affected pathways after RG108 treatment in HEI-OC1 cells. (C) Heat map of differentially expressed apoptosis-related genes in HEI-OC1 cells treated with cisplatin or RG108 + cisplatin. (D) The relative mRNA levels of the indicated genes were normalized to the GAPDH level in the HEI-OC1 cells treated with cisplatin or RG108 + cisplatin as determined by qRT-PCR. The results are expressed as mean ± SEM of three independent experiments. $^{****}P < 0.0001$ *vs.* Con; $^{\#\#\#\#}P < 0.0001$ *vs.* Cis.

cisplatin treatment, Western blot results revealed significantly reduced LRP1 amounts, while RG108 pretreatment increased LRP1 protein levels compared with the cisplatin group (Fig. 9B and C). It is widely accepted that the gene transcription rate controls mRNA expression, and promoter methylation is an important mechanism for decreasing mRNA transcription. Therefore, in order to verify the methylation status of *Lrp1*, we conducted a pyrosequencing assay. As depicted in Fig. 9D, RG108 effectively attenuated the hypermethylation levels of *Lrp1* in cisplatin-treated HEI-OC1 cells, which suggested that *Lrp1* upregulation might be caused by a low degree of promoter methylation. We finally examined whether LRP1 suppression

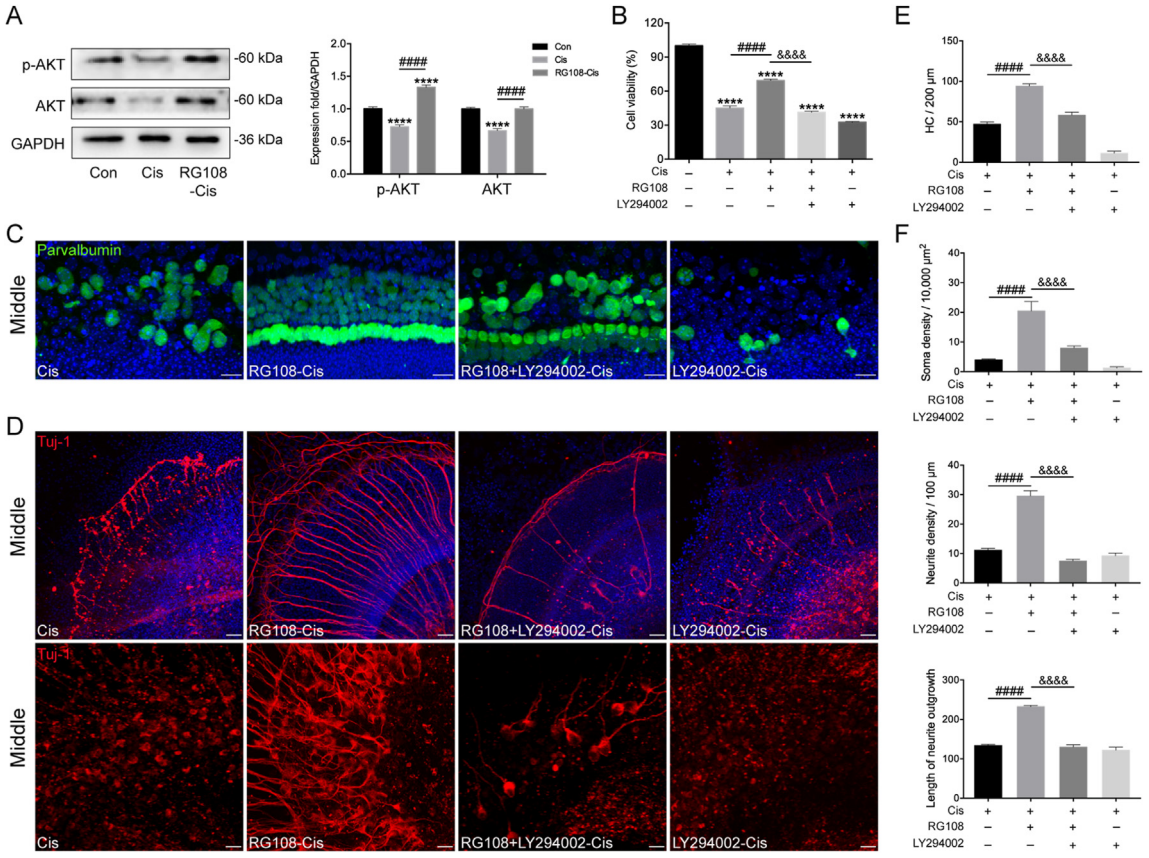

Figure 8 Effects of RG108 on PI3K/AKT pathway in HEI-OC1 cells undergoing cisplatin-induced damage. (A) Relative expression levels of AKT and phospho-AKT (p-AKT) by Western blot analysis. (B) HEI-OC1 cells were pretreated with RG108 and LY294002 for 2 h and then exposed to 30 μmol/L cisplatin for 24 h. Cell viability was determined by the CCK-8 assay. (C) and (D) Effects of LY294002 on RG108 mediated protection on cochlear HCs and SGNs following cisplatin challenge. Scale bars = 20 μm. (E) The illustration of HC counting (n = 8 cochleae). (F) Quantification analysis of SGN soma densities, neurite densities, and the length of neurite outgrowth from the middle turns of cochlear explants for all treatment conditions (n = 8 SGN explants). Data are presented as mean ± SEM. ****$P < 0.0001$, *vs.* Con; $^{\#\#\#\#}P < 0.0001$ *vs.* Cis; $^{\&\&\&\&}P < 0.0001$ *vs.* LY294002 + RG108-Cis.

diminished the protective effect of RG108. HEI-OC1 cells were transiently transfected with *Lrp1*-specific siRNAs (si1-*Lrp1*, si2-*Lrp1*, and si3-*Lrp1*), respectively. Q-PCR and Western blot showed that LRP1 was significantly silenced in si1-*Lrp1* and si3-*Lrp1*-treated cells (Fig. 9E–G). We found that RG108-induced promotion of cell viability was attenuated in si1-*Lrp1*-silenced cells (Fig. 9H). Moreover, increased AKT phosphorylation was undetectable in cells transfected with si1-*Lrp1*-specific siRNAs following RG108 treatment and cisplatin administration (Fig. 9I and J). These results suggest that knockdown of *Lrp1* could inhibit RG108-induced anti-apoptosis in HCs upon cisplatin damage *via* the PI3K/AKT pathway.

4. Discussion

Cisplatin represents a crucial chemotherapeutic agent broadly applied for solid tumors, whose use causes severe progressive and permanent hearing loss[38]. Many researchers have attempted to explore the mechanisms of cisplatin and ameliorate the associated ototoxicity. Recently, epigenetic changes, such as histone modifications, DNA methylation, and noncoding RNA profiles, have become exciting frontiers in studying inner ear development and hearing disorders[39–41]. For example, in an ototoxicity-induced hearing loss model, treatment with the HDAC inhibitor sodium butyrate reduces the expression of histone deacetylase 1 in HCs and protects against HC death and hearing loss by reducing oxidative stress[39,40]. Another specific HDAC inhibitor, TSA, was shown to alleviate the ototoxicity of cisplatin by upregulating genes associated with synaptic function and downregulating those involved in calcium and apoptosis signaling pathways[12]. DNA methylation is catalyzed by DNMTs and has critical functions in many biological processes, including gene expression, cell differentiation, and tumorigenesis[42,43]. In the auditory field, some reports showed that DNA methylation contributes to HC differentiation and regeneration[23–25]. However, its effect on ototoxic-induced HC death and the underlying mechanism remains undefined.

Here, we found that RG108, a novel non-nucleoside inhibitor of DNMTs, could alleviate cisplatin-induced death of HCs and SGNs in the mouse cochlea, *in vitro* and *in vivo*. Our study showed that RG108 has a beneficial effect similar to that previously used in the mouse motor neuron injury model[44]. It has been recognized that motor neuron apoptosis is related to the transient upregulation of DNMT activity and the increase of 5-mC in motor neurons. In contrast, treatment of mice with RG108 eliminated the injury-induced DNA methylation enhancement and motor neuron

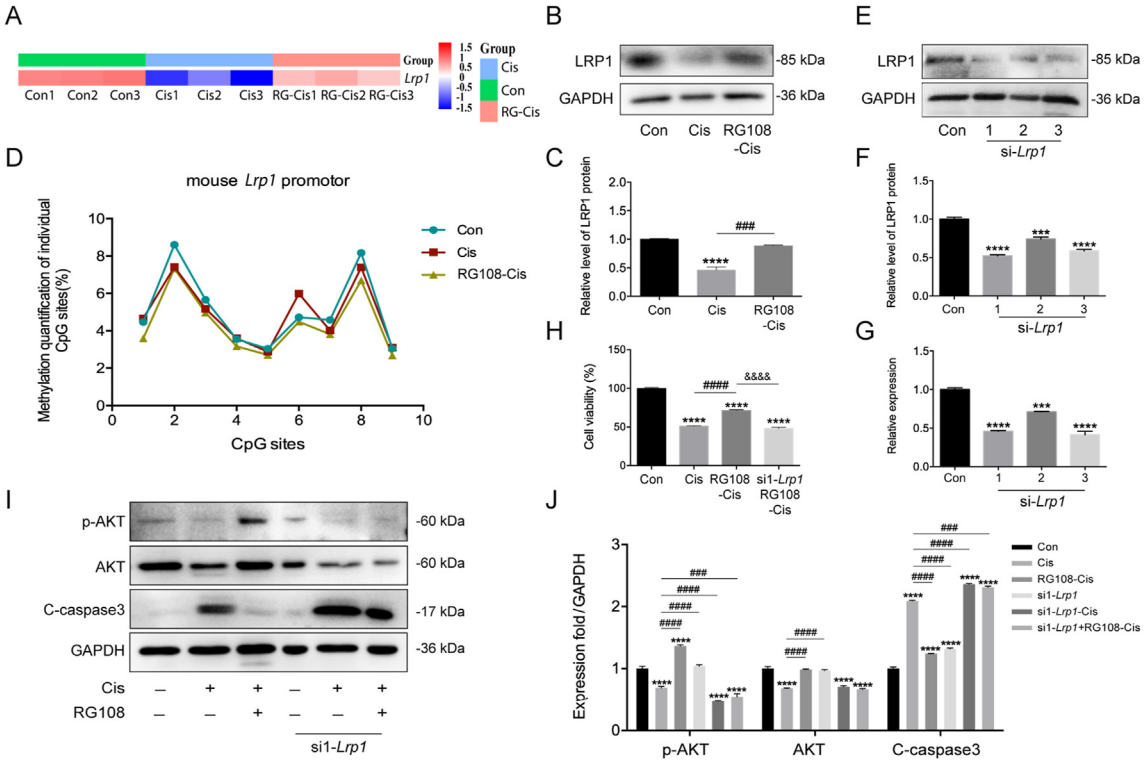

Figure 9 Role of LRP1 in RG108-mediated AKT activation in response to cisplatin stimulation. (A) Heat map of the expression level of *Lrp1* in Control, Cis, and RG108 + Cis groups. (B) and (C) The expressions of LRP1 were analyzed using Western blot analysis. (D) DNA methylation profile across the CpG was analyzed at the promoters of *Lrp1* in Control, Cis, and RG108 + Cis groups. (E) and (F) Representative Western blot was used to measure the protein expression level of LRP1 after transfection with siRNA-*Lrp1*. (G) mRNA expression levels of Lrp1 were analyzed by RT-qPCR. Western blot and RT-qPCR results confirmed that transfection of siRNA-*Lrp1* was successful. (H) Cell viability was determined by the CCK-8 assay. (I) and (J) The expressions of p-AKT, AKT, and cleaved-caspase3 (C-caspase3) were analyzed using Western blot analysis. Data are presented as mean ± SEM; $^{***}P < 0.001$, $^{****}P < 0.0001$ *vs.* Con; $^{\#\#\#}P < 0.001$, $^{\#\#\#\#}P < 0.0001$ *vs.* Cis; $^{\&\&\&\&}P < 0.0001$ *vs.* si1-*Lrp1* + RG108-Cis.

apoptosis. Our data are consistent with these studies, indicating that DNMT1 protein is upregulated in cisplatin-injured cochleae, and the immunoreactivity of 5-mC is increased in HCs. Pretreatment with RG108 could significantly down-regulate DNMT1 and block the increase of 5-mC immunoreactivity in HCs induced by cisplatin (Fig. S2).

Previous studies have reported that cisplatin administration decreases ribbon synapses that communicate the auditory signal generated by the IHCs to SGNs[45,46]. Ribbon synapses loss after cisplatin could alter the hearing transduction and contribute to the elevations of ABR thresholds which significantly impact hearing. Our results confirm those reports and demonstrate that ribbon synapses were significantly decreased following cisplatin treatment in mice. Since the ABR wave I amplitude and latency can be represented as indicators of activity at the spiral ganglion[47], we then analyzed ABR wave I amplitudes and latencies and found that administration of cisplatin significantly diminished amplitudes and elevated latencies compared to mice without cisplatin exposure. However, pretreatment with RG108 reversed the cisplatin-induced loss of ribbon synapses, decreased amplitudes, and increased latencies, indicating RG108 as a key mediator affecting cochlear synaptopathy. However, the detailed downstream mechanism that RG108 can prevent IHC synaptic loss after cisplatin injury needs to be further studied.

Apoptosis is a predominant cell death program induced by cisplatin in the cochlea[48]; meanwhile, RG108 was reported to exhibit anti-apoptotic effects in retinal pigment epithelial cells in response to oxidative stress[29]. Thus, we first examined the effect of RG108 on apoptosis. Our data revealed that TUNEL-positive cells were significantly more abundant upon cisplatin, indicating that cisplatin mainly causes HC and SGN death by inducing apoptosis, confirming previous findings[48]. However, TUNEL staining in the cochlea was less pronounced after treatment with RG108 plus cisplatin compared with the cisplatin alone group, indicating that RG108 mainly protects HCs and SGNs from cisplatin injury by inhibiting apoptosis.

An important mechanism of cisplatin-related ototoxicity is oxidative stress with the breakdown of oxidative metabolites in the mitochondria[49]. Mitochondrial dysfunction and free radicals (*e.g.*, ROS) accumulation are presumed to be the principal cellular mechanism underlying cisplatin-induced HC apoptosis[33]. Overproduction of ROS by cisplatin could overwhelm the redox balance, increase lipid peroxidation and inhibit the synthesis of endogenous antioxidants, promote mitochondrial cytochrome *c* release, and trigger the mitochondrial apoptosis pathway in HC, stria vascularis, marginal cell and spiral ganglion neuron apoptosis[33]. Thus, maintaining mitochondrial function and preventing ROS-accumulation-activated

caspase-mediated programmed cell death has been proposed as important strategies to avoid cisplatin-induced cytotoxicity[48,50]. In the current work, we established the HEI-OC1 cell model and explored the mechanism underlying the protective effect of RG108 in cisplatin-related cell damage. Following challenge with cisplatin, proapoptotic proteins such as BAX, BAD, and APAF1 were upregulated. In addition, MMP was reduced, with ROS overproduction accompanied by increased cytochrome *c* release following cisplatin challenge. These findings were consistent with previous work and suggested that cisplatin mainly exerts its effect *via* the mitochondrial apoptosis pathway[51]. However, the effects of RG108 on the downregulation of apoptotic proteins, MMP increase and ROS level reduction in HEI-OC1 cells reflected its protective effects on cisplatin-induced cell death, which is due, at least in part, to the inhibition of cisplatin-related DNA hypermethylation.

The primary role of the mitochondria is ATP production through OXPHOS reactions in the mitochondria and glycolysis in the cytosol for cell metabolism and biosynthesis. Mitochondrial membrane integrity is essential in mitochondrial OXPHOS. Damage to mitochondrial membrane integrity not only impairs mitochondrial OXPHOS, but also induces apoptosis. This study used extracellular flow analysis to measure mitochondrial respiratory function, and OCRs were recorded to further assess mitochondrial respiratory function (oxidative phosphorylation). This study demonstrated that cisplatin caused a marked reduction in oxidative phosphorylation in HEI-OC1 cells. The basal respiration rate was remarkably decreased in cisplatin-treated cells compared with controls. OCR-related ATP biosynthesis (assessed by oligomycin treatment) and maximum respiratory rate (evaluated by FCCP uncoupling) were significantly lower in cisplatin-treated cells than controls. RG108 treatment increased oxidative phosphorylation parameters such as basal respiration, ATP synthesis, maximum respiratory rates, preserving respiration capacity. Jointly, the above findings indicate cisplatin induces mitochondrial accumulation and dysfunction in HEI-OC1 cells.

In this study, 1009 genes were differentially expressed between the cisplatin and RG108+cisplatin groups by RNA-Seq. Pathway analysis of differentially expressed genes revealed that apoptosis-related pathways were the most altered following cisplatin treatment. KEGG analysis showed that the identified significant differential expressed genes were mainly involved in Axon guidance, Focal adhesion, RAP1, ECM-receptor interaction, and PI3K/AKT signaling, suggesting that RG108 might protect HEI-OC1 cells from cisplatin-related injury through a complex mechanism. Among these pathways, PI3K/AKT signaling had the highest enrichment, suggesting that this signaling pathway might play important roles in cisplatin-induced apoptosis. PI3K/AKT signaling controls many cell functions, including proliferation, cell cycle, survival, gene transcription, and other metabolic processes. Dysfunction of this signaling pathway causes metabolic, cardiovascular, and neurological diseases and leads to various types of cancer[52]. AKT has a central function in inducing cell survival by suppressing multiple downstream effectors of programmed cell death, inflammation, and mitochondria-produced ROS[53,54]. Recent studies suggested that PI3K/AKT signaling pathway participates in regulating sensory HC proliferation and survival[55,56]. PI3K/AKT signaling activity is decreased in HCs in response to various types of injury[57], and inhibition of this pathway reduce HC survival[58]. For example, dexamethasone activates the PI3K/AKT pathway and promotes HC survival against TNF-alpha-induced apoptosis for treating sensorineural hearing loss[59]. Kucharava et al.[60] reported that pasireotide protects cochlear HCs from gentamicin damage both *in vivo* and *in vitro* by upregulating the PI3K/AKT pathway. Consistent with these studies, our experiments demonstrated that the levels of phosphorylated AKT decreased in HEI-OC1 cells administered cisplatin, also accompanied by increased expression of proapoptotic proteins. This proposed PI3K/AKT pathway mechanism was further supported by the aggravation of cisplatin-induced ototoxicity in mouse HCs and SGNs by applying the PI3K/AKT inhibitor LY294002. Thus, the above findings confirmed PI3K/AKT signaling as a protective regulator responding to cisplatin exposure. More importantly, inhibition of PI3K/AKT signaling by LY294002 markedly reduced the protective effect of RG108 on cisplatin-induced damage in HEI-OC1 cells, demonstrated by reduced cell viability. These data thus suggest that RG108 could protect against cisplatin injury at least in part through activating PI3K/AKT signaling pathway. However, we cannot rule out that RG108 might protect against oxidative injury by regulating other signaling pathways, and these offer directions for future study.

Although PI3K/AKT signaling is implicated in HC survival, and its activation protects the inner ear HCs against harmful stimuli, the mechanisms are not fully defined. LRP1 represents a multifunctional receptor of low-density lipoproteins, which is known as a crucial scavenger receptor involved in the removal of cellular debris, as well as necrotic and apoptotic cells[61,62]. LRP1 can keep cells in an anti-inflammatory or anti-apoptotic status during injury induced by various insults[63,64]. For instance, a recent study showed that in a rat model of subarachnoid hemorrhage, LRP1 activation regulates M2 microglia polarization through Shc1/PI3K/AKT signaling pathway to reduce white matter injury and improve neurological function[37]. In our study, following cisplatin administration, we observed decreased LRP1 expression in HEI-OC1 cells, while RG108 pretreatment rescued this cisplatin caused decreased *Lrp1* expression. In addition, pyrosequencing analysis showed that cisplatin administration downregulated *Lrp1* expression by increasing the methylation status of the *Lrp1* promoter. But RG108 pretreatment could reduce the methylation status of *Lrp1*, suggesting that the transcriptional activity of *Lrp1* is associated with its DNA methylation level. To elucidate the role of LRP1, we silenced the expression of *Lrp1* in HEI-OC1 cells; as shown in Fig. 9, knockdown of *Lrp1* markedly enhanced cisplatin-mediated cell death, and it thus supports the notion that downregulation of *Lrp1* or increase of DNA methylation plays a positive role in apoptosis.

After confirming the role of LRP1 in cisplatin-mediated apoptosis, we next investigated the mechanisms underlying the functions of LRP1, and we demonstrated that LRP1 deficiency promoted apoptosis *via* suppression of AKT activation. The results indicated that LRP1 exerts anti-apoptotic effects through PI3K/AKT signaling, corroborating previous findings[37]. Moreover, *Lrp1* knockdown by siRNA significantly reversed the anti-apoptotic effects of RG108 under cisplatin injury, as indicated by CCK-8. Increased phosphorylation of AKT was remarkably decreased in cells after transfection with *Lrp1*-specific siRNA following RG108 pretreatment compared with cells administered cisplatin as examined by Western blot. These findings strongly support the notion that LRP1 is involved in the protective effects of RG108 on HCs upon cisplatin damage through the PI3K/AKT pathway. In order to clarify whether hypermethylation of the *Lrp1* promoter directly induces apoptosis in HCs, additional studies to evaluate

the methylation and demethylation of the *Lrp1* promoter are needed. The CRISPR system accurately and effectively mutates genes through sgRNA and CAS. The gene-editing method could accurately identify hypermethylation sites in genes and demonstrate the effects of promoter methylation. In the future, the CRISPR system may be an appropriate method to elucidate the methylation function of LRP1.

5. Conclusions

Overall, the current work showed that RG108 could reduce HC death, alleviate neuron loss, and improve hearing function after cisplatin administration. Moreover, our results suggested that RG108 treatment could reduce ROS accumulation and inhibit apoptosis, which is mediated, at least partially, through LRP1−PI3K/AKT signaling pathway. Collectively, our findings provide clues that RG108 may represent an attractive therapeutic epigenetic agent for preventing and treating hearing loss in the clinic.

Acknowledgments

The authors would like to thank Yalin Huang for help with the confocal microscope. This work was supported by grants from the National Key R&D Program of China (No. 2017YFA0103900), the National Natural Science Foundation of China (Nos. 82071045, 81870728, 81830029, and 81970875), and Shanghai Rising-Star Program (19QA1401800).

Author contributions

Yingzi He, Zhiwei Zheng, and Chang Liu conceived the experiments, performed the majority of experiments, analyzed the data, and drafted the paper. Wen Li and Liping Zhao performed partial experiments and acquired the data. Huawei Li designed the study, supervised the experiments, and gave the final approval of the manuscript. Guohui Nie designed the study, analyzed the data, wrote a part of the paper, and revised the paper. All authors read and approved the manuscript as submitted.

Conflicts of interest

The authors declare no conflicts of interest.

Appendix A. Supporting information

Supporting data to this article can be found online at https://doi.org/10.1016/j.apsb.2021.11.002.

References

1. Rybak LP, Whitworth CA, Mukherjea D, Rarakumar V. Mechanisms of cisplatin-induced ototoxicity and prevention. *Hear Res* 2007;**226**:157−67.
2. Karasawa T, Steyger PS. An integrated view of cisplatin-induced nephrotoxicity and ototoxicity. *Toxicol Lett* 2015;**237**:219−27.
3. Kim YJ, Kim J, Tian C, Lim HJ, Kim YS, Chung JH, et al. Prevention of cisplatin-induced ototoxicity by the inhibition of gap junctional intercellular communication in auditory cells. *Cell Mol Life Sci* 2014;**71**:3859−71.
4. Rybak LP, Mukherjea D, Jajoo S, Ramkumar V. Cisplatin ototoxicity and protection: clinical and experimental studies. *Tohoku J Exp Med* 2009;**219**:177−86.
5. Mohan S, Smyth BJ, Namin A, Phillips G, Gratton MA. Targeted amelioration of cisplatin-induced ototoxicity in guinea pigs. *Otolaryngol Head Neck Surg* 2014;**151**:836−9.
6. Dickey DT, Muldoon LL, Doolittle ND, Peterson DR, Kraemer DF, Neuwelt EA. Effect of *N*-acetylcysteine route of administration on chemoprotection against cisplatin-induced toxicity in rat models. *Cancer Chemother Pharmacol* 2008;**62**:235−41.
7. Choe WT, Chinosornvatana N, Chang KW. Prevention of cisplatin ototoxicity using transtympanic *N*-acetylcysteine and lactate. *Otol Neurotol* 2004;**25**:910−5.
8. Wimmer C, Mees K, Stumpf T, Welsch U, Reichel O, Suckfull M. Round window application of D-methionine, sodium thiosulfate, brain-derived neurotrophic factor, and fibroblast growth factor-2 in cisplatin-induced ototoxicity. *Otol Neurotol* 2004;**25**:33−40.
9. Kouzarides T. Chromatin modifications and their function. *Cell* 2007;**128**:693−705.
10. Jones PA. Functions of DNA methylation: islands, start sites, gene bodies and beyond. *Nat Rev Genet* 2012;**13**:484−92.
11. Zheng BN, Ding CH, Chen SJ, Zhu K, Shao J, Feng J, et al. Targeting PRMT5 activity inhibits the malignancy of hepatocellular carcinoma by promoting the transcription of HNF4alpha. *Theranostics* 2019;**9**:2606−17.
12. Wang P, Zhang P, Huang J, Li M, Chen X. Trichostatin A protects against cisplatin-induced ototoxicity by regulating expression of genes related to apoptosis and synaptic function. *Neurotoxicology* 2013;**37**:51−62.
13. Yu H, Lin Q, Wang Y, He Y, Fu S, Jiang H, et al. Inhibition of H3K9 methyltransferases G9a/GLP prevents ototoxicity and ongoing hair cell death. *Cell Death Dis* 2013;**4**:e506.
14. He YZ, Li W, Zheng ZW, Zhao LP, Li WY, Wang YF, et al. Inhibition of protein arginine methyltransferase 6 reduces reactive oxygen species production and attenuates aminoglycoside- and cisplatin-induced hair cell death. *Theranostics* 2020;**10**:133−50.
15. Jones PA, Takai D. The role of DNA methylation in mammalian epigenetics. *Science* 2001;**293**:1068−70.
16. Jaenisch R, Bird A. Epigenetic regulation of gene expression: how the genome integrates intrinsic and environmental signals. *Nat Genet* 2003;**33**:245−54.
17. Bird AP. Cpg-rich islands and the function of DNA methylation. *Nature* 1986;**321**:209−13.
18. Turek-Plewa J, Jagodzinski PP. The role of mammalian DNA methyltransferases in the regulation of gene expression. *Cell Mol Biol Lett* 2005;**10**:631−47.
19. Robertson KD. DNA methylation, methyltransferases, and cancer. *Oncogene* 2001;**20**:3139−55.
20. Okano M, Bell DW, Haber DA, Li E. DNA methyltransferases Dnmt3a and Dnmt3b are essential for *de novo* methylation and mammalian development. *Cell* 1999;**99**:247−57.
21. Sanz LA, Kota SK, Feil R. Genome-wide DNA demethylation in mammals. *Genome Biol* 2010;**11**:110.
22. Guo F, Li XL, Liang D, Li T, Zhu P, Guo HS, et al. Active and passive demethylation of male and female pronuclear DNA in the mammalian zygote. *Cell Stem Cell* 2014;**15**:447−58.
23. Zhou Y, Hu ZQ. Epigenetic DNA demethylation causes inner ear stem cell differentiation into hair cell-like cells. *Front Cell Neurosci* 2016;**10**:185.
24. Zhou Y, Hu ZQ. Genome-wide demethylation by 5-aza-2′-deoxycytidine alters the cell fate of stem/progenitor cells. *Stem Cell Rev Rep* 2015;**11**:87−95.
25. Deng X, Liu ZJ, Li XY, Zhou Y, Hu ZQ. Generation of new hair cells by DNA methyltransferase (Dnmt) inhibitor 5-azacytidine in a chemically-deafened mouse model. *Sci Rep* 2019;**9**:7997.
26. Fahy J, Jeltsch A, Arimondo PB. DNA methyltransferase inhibitors in cancer: a chemical and therapeutic patent overview and selected clinical studies. *Expert Opin Ther Pat* 2012;**22**:1427−42.

27. Siedlecki P, Boy RG, Musch T, Brueckner B, Suhai S, Lyko F, et al. Discovery of two novel, small-molecule inhibitors of DNA methylation. *J Med Chem* 2006;**49**:678−83.
28. Stresemann C, Lyko F. Modes of action of the DNA methyltransferase inhibitors azacytidine and decitabine. *Int J Cancer* 2008;**123**:8−13.
29. Tokarz P, Kaarniranta K, Blasiak J. Inhibition of DNA methyltransferase or histone deacetylase protects retinal pigment epithelial cells from DNA damage induced by oxidative stress by the stimulation of antioxidant enzymes. *Eur J Pharmacol* 2016;**776**:167−75.
30. Teitz T, Fang J, Goktug AN, Bonga JD, Diao SY, Hazlitt RA, et al. CDK2 inhibitors as candidate therapeutics for cisplatin-and noise-induced hearing loss. *J Exp Med* 2018;**215**:1187−203.
31. Fears CY, Grammer JR, Stewart Jr JE, Annis DS, Mosher DF, Bornstein P, et al. Low-density lipoprotein receptor-related protein contributes to the antiangiogenic activity of thrombospondin-2 in a murine glioma model. *Cancer Res* 2005;**65**:9338−46.
32. Bolger AM, Lohse M, Usadel B. Trimmomatic: a flexible trimmer for Illumina sequence data. *Bioinformatics* 2014;**30**:2114−20.
33. Dehne N, Lautermann J, Petrat F, Rauen U, de Groot H. Cisplatin ototoxicity: involvement of iron and enhanced formation of superoxide anion radicals. *Toxicol Appl Pharm* 2001;**174**:27−34.
34. Wu M, Neilson A, Swift AL, Moran R, Tamagnine J, Parslow D, et al. Multiparameter metabolic analysis reveals a close link between attenuated mitochondrial bioenergetic function and enhanced glycolysis dependency in human tumor cells. *Am J Physiol Cell Physiol* 2007;**292**:C125−36.
35. Zheng ZW, Wang YF, Yu HQ, Li W, Wu JF, Cai CF, et al. Salvianolic acid B inhibits ototoxic drug-induced ototoxicity by suppression of the mitochondrial apoptosis pathway. *J Cell Mol Med* 2020;**24**:6883−97.
36. Chuang TY, Guo Y, Seki SM, Rosen AM, Johanson DM, Mandell JW, et al. LRP1 expression in microglia is protective during CNS autoimmunity. *Acta Neuropathol Commun* 2016;**4**:68.
37. Peng JH, Pang JW, Huang L, Enkhjargal B, Zhang TY, Mo J, et al. LRP1 activation attenuates white matter injury by modulating microglial polarization through Shc1/PI3K/Akt pathway after subarachnoid hemorrhage in rats. *Redox Biol* 2019;**21**:101121.
38. Ruggiero A, Trombatore G, Triarico S, Arena R, Ferrara P, Scalzone M, et al. Platinum compounds in children with cancer: toxicity and clinical management. *Anticancer Drugs* 2013;**24**:1007−19.
39. Chen FQ, Schacht J, Sha SH. Aminoglycoside-induced histone deacetylation and hair cell death in the mouse cochlea. *J Neurochem* 2009;**108**:1226−36.
40. Drottar M, Liberman MC, Ratan RR, Roberson DW. The histone deacetylase inhibitor sodium butyrate protects against cisplatin-induced hearing loss in guinea pigs. *Laryngoscope* 2006;**116**:292−6.
41. Yang DH, Xie J, Liu K, Peng Z, Guo JY, Yu SK, et al. The histone deacetylase inhibitor sodium butyrate protects against noise-induced hearing loss in Guinea pigs. *Neurosci Lett* 2017;**660**:140−6.
42. Uysal F, Akkoyunlu G, Ozturk S. Dynamic expression of DNA methyltransferases (DNMTs) in oocytes and early embryos. *Biochimie* 2015;**116**:103−13.
43. Yan F, Shen N, Pang JX, Zhao N, Zhang YW, Bode AM, et al. A vicious loop of fatty acid-binding protein 4 and DNA methyltransferase 1 promotes acute myeloid leukemia and acts as a therapeutic target. *Leukemia* 2018;**32**:865−73.
44. Chestnut BA, Chang Q, Price A, Lesuisse C, Wong M, Martin LJ. Epigenetic regulation of motor neuron cell death through DNA methylation. *J Neurosci* 2011;**31**:16619−36.
45. Borse V, Al Aameri RFH, Sheehan K, Sheth S, Kaur T, Mukherjea D, et al. Epigallocatechin-3-gallate, a prototypic chemopreventative agent for protection against cisplatin-based ototoxicity. *Cell Death Dis* 2017;**8**:e2921.
46. Ghosh S, Sheth S, Sheehan K, Mukherjea D, Dhukhwa A, Borse V, et al. The endocannabinoid/cannabinoid receptor 2 system protects against cisplatin-induced hearing loss. *Front Cell Neurosci* 2018;**12**:271.
47. Kujawa SG, Liberman MC. Adding insult to injury: cochlear nerve degeneration after "Temporary" noise-induced hearing loss. *J Neurosci* 2009;**29**:14077−85.
48. Sheth S, Mukherjea D, Rybak LP, Ramkumar V. Mechanisms of cisplatin-induced ototoxicity and otoprotection. *Front Cell Neurosci* 2017;**11**:338.
49. Schacht J, Talaska AE, Rybak LP. Cisplatin and aminoglycoside antibiotics: hearing loss and its prevention. *Anat Rec* 2012;**295**:1837−50.
50. Rybak LP, Kelly T. Ototoxicity: bioprotective mechanisms. *Curr Opin Otolaryngol Head Neck Surg* 2003;**11**:328−33.
51. Rybak LP, Mukherjea D, Ramkumar V. Mechanisms of cisplatin-induced ototoxicity and prevention. *Semin Hear* 2019;**40**:197−204.
52. Tokunaga E, Oki E, Egashira A, Sadanaga N, Morita M, Kakeji Y, et al. Deregulation of the Akt pathway in human cancer. *Curr Cancer Drug Targets* 2008;**8**:27−36.
53. Kennedy SG, Wagner AJ, Conzen SD, Jordan J, Bellacosa A, Tsichlis PN, et al. The PI3-kinase/Akt signaling pathway delivers an anti-apoptotic signal. *Gene Dev* 1997;**11**:701−13.
54. Orike N, Middleton G, Borthwick E, Buchman V, Cowen T, Davies AM. Role of PI3-kinase, Akt and Bcl-2-related proteins in sustaining the survival of neurotrophic factor-independent adult sympathetic neurons. *J Cell Biol* 2001;**154**:995−1005.
55. Aburto MR, Magarinos M, Leon Y, Varela-Nieto I, Sanchez-Calderon H. AKT signaling mediates IGF-I survival actions on otic neural progenitors. *PLoS One* 2012;**7**:e30790.
56. Brand Y, Levano S, Radojevic V, Naldi AM, Setz C, Ryan AF, et al. All Akt isoforms (Akt1, Akt2, Akt3) are involved in normal hearing, but only Akt2 and Akt3 are involved in auditory hair cell survival in the mammalian inner ear. *PLoS One* 2015;**10**:e0121599.
57. Selivanova O, Brieger J, Heinrich UR, Mann W. Akt and c-Jun N-terminal kinase are regulated in response to moderate noise exposure in the cochlea of guinea pigs. *ORL J Otorhinolaryngol Relat Spec* 2007;**69**:277−82.
58. Chung WH, Pak K, Lin B, Webster N, Ryan AF. A PI3K pathway mediates hair cell survival and opposes gentamicin toxicity in neonatal rat organ of Corti. *J Assoc Res Otolaryngol* 2006;**7**:373−82.
59. Haake SM, Dinh CT, Chen S, Eshraghi AA, Van De Water TR. Dexamethasone protects auditory hair cells against TNFalpha-initiated apoptosis *via* activation of PI3K/Akt and NFkappaB signaling. *Hear Res* 2009;**255**:22−32.
60. Kucharava K, Sekulic-Jablanovic M, Horvath L, Bodmer D, Petkovic V. Pasireotide protects mammalian cochlear hair cells from gentamicin ototoxicity by activating the PI3K−Akt pathway. *Cell Death Dis* 2019;**10**:110.
61. Fernandez-Castaneda A, Arandjelovic S, Stiles TL, Schlobach RK, Mowen KA, Gonias SL, et al. Identification of the low density lipoprotein (LDL) receptor-related protein-1 interactome in central nervous system myelin suggests a role in the clearance of necrotic cell debris. *J Biol Chem* 2013;**288**:4538−48.
62. Gardai SJ, McPhillips KA, Frasch SC, Janssen WJ, Starefeldt A, Murphy-Ullrich JE, et al. Cell-surface calreticulin initiates clearance of viable or apoptotic cells through trans-activation of LRP on the phagocyte. *Cell* 2005;**123**:321−34.
63. Campana WM, Li XQ, Dragojlovic N, Janes J, Gaultier A, Gonias SL. The low-density lipoprotein receptor-related protein is a pro-survival receptor in Schwann cells: possible implications in peripheral nerve injury. *J Neurosci* 2006;**26**:11197−207.
64. Zurhove K, Nakajima C, Herz J, Bock HH, May P. Gamma-secretase limits the inflammatory response through the processing of LRP1. *Sci Signal* 2008;**1**:ra15.